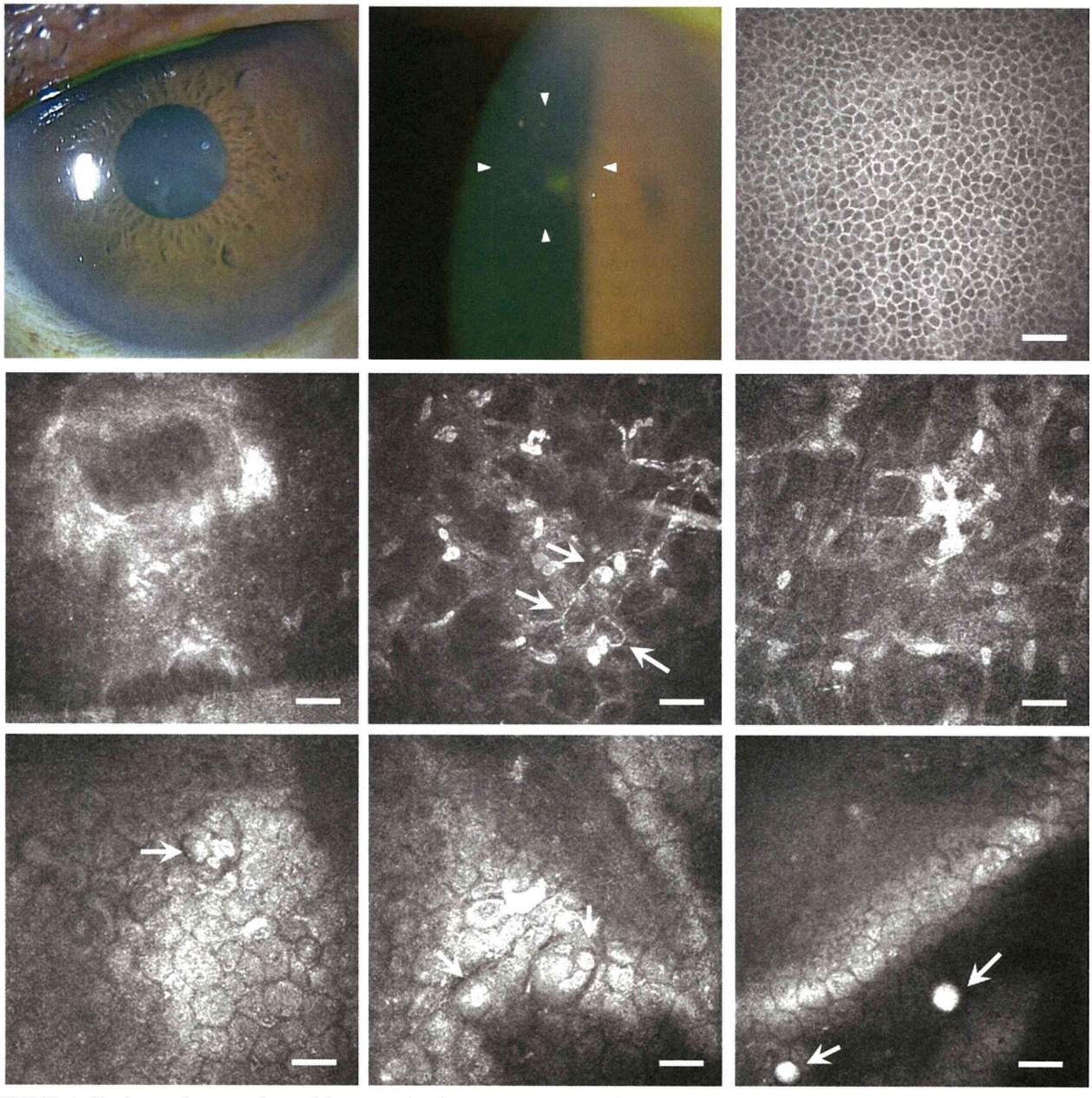

FIGURE 4. Slit-lamp photographs and laser confocal microscopy scans from a patient with cytomegalovirus corneal endotheliitis (Patient 2). (Top left) Slit-lamp photograph of the left cornea of Patient 2 at an initial visit to the hospital. (Top center) Coin-shaped lesions and disciform edema were observed in the upper temporal region (arrowheads). (Top right) Epithelial basal cell layer in the center of the cornea demonstrating normal results by Heidelberg Retina Tomograph 2 Rostock Cornea Module (HRT 2-RCM). Bar = 50 μm. (Second row left) Increased intensity of Bowman layer with highly reflective tiny dots were observed. (Second row middle) Aberrant shape of subepithelial nerves was observed (arrows). (Second row right) Subepithelial opacity with increased reflectivity of keratocytes and highly reflective needle-shaped bodies were noted. (Bottom middle and left) Owl eye morphologic features were detectable by HRT 2-RCM (arrows). Endothelial cell density was 1730 cells/mm^2. (Bottom right) Highly reflective round bodies were noted (arrows).

tative clinical diagnosis of CMV corneal endotheliitis, which may prevent further endothelial cell loss that may happen while waiting for the PCR results. However, one limitation of confocal microscopic examination is that the device may not be useful for patients with severe corneal stromal edema, because this may prevent visualization of the corneal endothelium layer.

We hypothesized that aggregates of highly reflective round bodies visualized by HRT2-RCM may correspond to the coin-shaped lesions observed by slit-lamp biomicroscopy.

That is, the coin-shaped lesions may correspond to necrotic and aggregated corneal endothelial cells that are infected with CMV. The fact that the owl eye morphologic features are visualized better around the area of coin-shaped lesions, but are not seen uniformly in the endothelial cell layer (unpublished observation), also may support this hypothesis.

In conclusion, in vivo laser confocal microscopy is capable of identifying characteristic corneal microstructural changes related to CMV corneal endotheliitis. Specifically, owl eye morphologic features and highly reflective round bodies may be useful adjuncts for the noninvasive diagnosis of CMV corneal endotheliitis. Additionally, HRT2-RCM may be useful for monitoring the therapeutic effects of systemic and topical antiviral drugs and may provide information regarding the timing for discontinuing medications without multiple anterior chamber tap. Further studies using a large number of patients and including other types of endothelial diseases are required to elucidate fully the clinical significance of owl eye morphologic features in CMV endotheliitis.

PUBLICATION OF THIS ARTICLE WAS SUPPORTED BY GRANT 10103447 FROM THE INTRACTABLE DISEASE TREATMENT Research Program; the Ministry of Health, Labour and Welfare, Tokyo, Japan; and Grant-in-Aid for Scientific Research 22591934 from Kakenhi, Tokyo, Japan. The sponsors or funding organizations had no role in the design or conduct of this research. The corresponding investigator (A.K.) has full access to all data in the study and takes responsibility for the integrity of the data and accuracy of the data analysis. The authors indicate no financial conflict of interest. Involved in Design (A.K.) and conduct (H.Y., A.K., K.N.) of study; Collection, management, analysis, and interpretation of the data (H.Y., A.K.); and Preparation, review, or approval of manuscript (T.H., K.S.). This prospective study was approved by the Ethical Committee of Kanazawa University Graduate School of Medical Science and followed the tenets of the Declaration of Helsinki.

REFERENCES

1. Khodadoust AA, Attarzadeh A. Presumed autoimmune corneal endotheliopathy. Am J Ophthalmol 1982;93(6):718–722.
2. Ohashi Y, Yamamoto S, Nishida K, et al. Demonstration of herpes simplex virus DNA in idiopathic corneal endotheliopathy. Am J Ophthalmol 1991;112(4):419–423.
3. Maudgal PC, Missotten L, De Clercq E, Descamps J. Varicella-zoster virus in the human corneal endothelium: a case report. Bull Soc Belge Ophthalmol 1980;190:71–86.
4. Singh K, Sodhi PK. Mumps-induced corneal endotheliitis Cornea 2004;23(4):400–402.
5. Koizumi N, Yamasaki K, Kawasaki S, et al. Cytomegalovirus in aqueous humor from an eye with corneal endotheliitis. Am J Ophthalmol 2006;141(3):564–565.
6. Koizumi N, Suzuki T, Uno T, et al. Cytomegalovirus as an etiologic factor in corneal endotheliitis. Ophthalmology 2008;115(2):292–297.
7. Sonoyama H, Araki-Sasaki K, Osakabe Y, et al. Detection of cytomegalovirus DNA from cytomegalovirus corneal endotheliitis after penetrating keratoplasty. Cornea 2010;29(6):683–685.
8. Wang SC, Tsai IL, Lin HC, et al. Recurrent cytomegalovirus corneal endotheliitis after penetrating keratoplasty. Eur J Ophthalmol 2010;20(2):457–459.
9. Cavanagh HD, Petroll WM, Alizadeh H, et al. Clinical and diagnostic use of in vivo confocal microscopy in patients with corneal disease. Ophthalmology 1993;100(10):1444–1454.
10. Bohnke M, Masters BR. Confocal microscopy of the cornea. Prog Retin Eye Res 1999;18(5):553–628.
11. Kaufman SC, Musch DC, Belin MW, et al. Confocal microscopy: a report by the American Academy of Ophthalmology. Ophthalmology 2004;111(7):396–406.
12. Kobayashi A, Sugiyama K. In vivo corneal confocal microscopic findings of palisades of Vogt and its underlying limbal stroma. Cornea 2005;24(4):435–437.
13. Kobayashi A, Sugiyama K, Huang AJ. In vivo confocal microscopy in patients with central cloudy dystrophy of Francois. Arch Ophthalmol 2004;122(11):1676–1679.
14. Zhivov A, Stachs O, Kraak R, et al. In vivo confocal microscopy of the ocular surface. Ocul Surf 2006;4(2):81–93.
15. Kobayashi A, Yokogawa H, Sugiyama K. In vivo laser confocal microscopy of Bowman's layer of the cornea. Ophthalmology 2006;113(12):2203–2208.
16. Kobayashi A, Sugiyama K. In vivo laser confocal microscopy findings for Bowman's layer dystrophies (Thiel-Behnke and Reis-Bücklers corneal dystrophies). Ophthalmology 2007;114(1):69–75.
17. Heidelberg Engineering. Heidelberg Retina Tomograph 2 (Rostock Cornea Module) Operating Instructions of software version 1.1. Dossenheim, Germany: Heidelberg Engineering; 2004.
18. Nidek Technologies. Confoscan 2: operator's manual. Vigonza, Italy: Nidek Technologies; 2001.
19. Shiraishi A, Hara Y, Takahashi M, et al. Demonstration of "owl's eye" morphology by confocal microscopy in a patient with presumed cytomegalovirus corneal endotheliitis. Am J Ophthalmol 2007;143(4):715–717.
20. Kobayashi A, Mawatari Y, Yokogawa H, Sugiyama K. In vivo laser confocal microscopy after Descemet stripping with automated endothelial keratoplasty. Am J Ophthalmol 2008;145(6):977–985.
21. Kobayashi A, Yokogawa H, Sugiyama K. In vivo laser confocal microscopy after non-Descemet's stripping automated endothelial keratoplasty. Ophthalmology 2009;116(7):1306–1313.
22. Efron N. Contact lens-induced changes in the anterior eye as observed in vivo with the confocal microscope. Prog Retin Eye Res 2007;26(4):398–436.
23. Kobayashi A, Maeda A, Sugiyama K. In-vivo confocal microscopy in the acute phase of corneal inflammation. Ophthalmic Surg Lasers Imaging 2003;34(5):433–436.
24. Herriot R, Gray ES. Images in clinical medicine: owl's-eye cells. N Engl J Med 1994;331(10):649.
25. Wertheim MS, Mathers WD, Planck SJ, et al. In vivo confocal microscopy of keratic precipitates. Arch Ophthalmol 2004;122(12):1773–1781.
26. Mocan MC, Kadayifcilar S, Irkec M. Keratic precipitate morphology in uveitic syndromes including Behçet's disease as evaluated with in vivo confocal microscopy. Eye 2009;23(5):1221–1227.

Jpn J Ophthalmol 2011;55:98–102
DOI 10.1007/s10384-010-0916-8

CLINICAL INVESTIGATION

Intraocular Pressure After Descemet's Stripping and Non-Descemet's Stripping Automated Endothelial Keratoplasty

Yoshiro Mawatari, Akira Kobayashi, Hideaki Yokogawa, and Kazuhisa Sugiyama

Department of Ophthalmology, Kanazawa University Graduate School of Medical Science, Kanazawa, Japan

Abstract

Purpose: To evaluate the effect on intraocular pressure (IOP) of increased corneal thickness after Descemet's stripping automated endothelial keratoplasty (DSAEK) and of non-Descemet's stripping automated endothelial keratoplasty (nDSAEK) as measured by four different techniques.

Methods: Twenty-four eyes (22 patients; mean age, 74.0 years) with successful DSAEK (11 eyes) or nDSAEK (13 eyes) treatment at least 3 months prior to testing were enrolled. IOP was measured with Goldmann applanation tonometry (GAT), dynamic contour tonometry (DCT), pneumatonometry, and Tono-Pen XL (Tonopen). Central corneal thickness (CCT) was measured by ultrasonic pachymetry. These data were used for statistical analysis.

Results: Mean IOP measured by GAT, DCT, pneumatonometry, and Tonopen was 14.4, 13.9, 11.2, and 13.2 mmHg, respectively, in the DSAEK group; and 15.0, 14.4, 12.5, and 14.4 mmHg, respectively, in the nDSAEK group. Correlations between IOP and CCT were not statistically significant in either group. Pressure measured by pneumatonometry was significantly and consistently lower than that obtained by the other three methods.

Conclusion: For both DSAEK and nDSAEK, IOP readings by the four tonometers seem to be unrelated to artificially thickened corneas. **Jpn J Ophthalmol** 2011;55:98–102 © Japanese Ophthalmological Society 2011

Keywords: DSAEK, endothelial keratoplasty, intraocular pressure, nDSAEK

Introduction

Over the past several years, new surgical techniques have been reported for bullous keratopathy that replace only the dysfunctional posterior portion of the cornea through a scleral pocket incision.[1–5] These techniques completely eliminate surface corneal incisions and sutures, maintain much of the cornea's structural integrity, and induce minimal refractive changes, suggesting distinct advantages over standard penetrating keratoplasty. Recently, preparation of donor tissue for this type of procedure, termed endothelial keratoplasty, has been made easier with the utilization of an automated microkeratome. The enhanced surgical procedure with the automated microkeratome is known as Descemet's stripping automated endothelial keratoplasty (DSAEK).[4,6] Recently, we reported a successful modification of DSAEK without Descemet's membrane peeling for bullous keratopathies secondary to Argon laser iridotomy; we termed the modified procedure non-Descemet's stripping automated endothelial keratoplasty (nDSAEK).[7,8]

After both DSAEK and nDSAEK surgery, corneal thickness inevitably increases owing to the addition of the

Received: May 10, 2010 / Accepted: November 5, 2010
Correspondence and reprint requests to: Akira Kobayashi, Department of Ophthalmology, Kanazawa University Graduate School of Medical Science, 13-1 Takara-machi, Kanazawa, Ishikawa 920-8641, Japan
e-mail: kobaya@kenroku.kanazawa-u.ac.jp

Originally presented at the Association for Research in Vision and Ophthalmology Annual Meeting, 2 May 2010, Fort Lauderdale, Florida, USA.

donor graft. Therefore, there is a possibility that intraocular pressure (IOP) measurement methods dependent on normal corneal thickness, such as Goldmann applanation tonometry (GAT), may produce less accurate readings.

The purpose of the current study was to evaluate the effect of both post-DSAEK and nDSAEK increased corneal thickness on IOP readings obtained with one of the following four techniques: GAT, dynamic contour tonometry (DCT), non-contact pneumatonometry, and miniaturized digital electronic tonometry (Tono-Pen XL, or Tonopen).

Patients and Methods

This prospective, cross-sectional study was approved by the Ethical Committee of Kanazawa University Graduate School of Medical Science and complied with the tenets of the Declaration of Helsinki. We evaluated 24 eyes (22 patients: 6 men, 16 women; mean age, 74.0 years) that had undergone either successful DSAEK (11 eyes) or nDSAEK (13 eyes) treatment at least 3 months prior to testing (mean duration, 327.0 ± 167.4 days; range, 103–621 days). The causes of the corneal edema were post-argon laser iridotomy (17/24, 70.8%), followed by endothelitis (3/24, 12.5%), Fuchs dystrophy (2/24, 8.3%), pseudophakia (1/24, 4.2%), and pseudoexofoliation (1/24, 4.2%). Pseudoexofoliation syndrome is known to cause endothelial cell loss.[9] None of the patients had a previous glaucoma procedure. All surgeries were performed by a single surgeon (A. K.). DSAEK and nDSAEK procedures are described in detail by Kobayashi and Yokogawa and colleagues.[7,8,10] In brief, donor grafts for all 24 eyes were prepared with a microkeratome (ALTK Cbm, Moria, Antony, France) equipped with a 300-μm head and an 8.0-mm-diameter punch (Barron donor cornea punch, Katena Products, Denville, NJ, USA). In 14 of the 24 cases, simultaneous cataract procedures (phacoemulsification and intraocular lens implantation) were performed just prior to both the DSAEK and nDSAEK surgery. In the nDSAEK procedures, the Descemet's membrane scoring and stripping process was totally eliminated.

We excluded patients with clinically detectable corneal edema or other active corneal pathology such as an epithelial defect or infection. Each patient enrolled in the study underwent a comprehensive anterior segment evaluation. All corneas evaluated in this study were crystal clear, and none of the participants had corneal edema clinically detectable by slit-lamp biomicroscopy at the time of study evaluation.

All IOP measurements were performed by one of two authors (A. K., H. Y.). Pressure was measured with Goldmann applanation tonometry (GAT) and dynamic contour tonometry (DCT: PASCAL, Swiss Microtechnology, Zurich, Switzerland),[11,12] pneumatonometry (TX-F, Canon, Tokyo, Japan), and Tonopen (Tono-Pen XL; Mentor Massachusetts, Norwell, MA, USA). Measuring was conducted in the following sequence: pneumatonometry, GAT, DCT, and Tonopen. The time interval between measurements using each technique was about 5 min. Two measurements on average were obtained with each technique; additional measurements were performed only if the difference between the first and second measurements exceeded 2 mmHg. For DCT measurement, a DCT module was mounted onto a slit-lamp biomicroscope (30SL-M, Carl Zeiss Japan, Tokyo, Japan), after which a disposable sensor cap was attached. After the cornea was anesthetized, the measuring tip was aligned so that the pressure sensor was centered within the contact zone for 3–5 s. IOP readings and the quality of the measurement were displayed on the digital screen; a reading of quality (Q) 1 to Q3 (with Q1 the best) was considered acceptable. Poor readings (rated Q4 to Q5) were discarded, and the pressure was measured again. Central corneal thickness (CCT) was measured by ultrasonic pachymetry (DGH 500; DGH Technology, Exton, PA, USA). Three measurements on average were used for the analysis of total corneal thickness.

Bland-Altman plots were examined to assess agreement between each pair of measurement methods.[13] The mean pressure measurement for each pair of methods was plotted on the x axis, with the difference in measurements between methods plotted on the y axis. In brief, if the two measurements were nearly identical, the mean difference would be close to zero. In addition, correlations between CCT and pressure measurements were assessed.

Descriptive statistics were expressed as mean ± standard deviation (SD). For all analyses, P values of less than 0.05 were considered statistically significant. Sample size calculation was performed as described previously,[14] when IOP measured by DCT and GAT was compared.

Results

Pressure was consistently measured with good quality using DCT (all patients scored Q3 on the quality scale). In the DSAEK group, mean pressure measured by GAT was 14.4 ± 3.6 mmHg, by DCT 13.9 ± 3.0, by pneumatonometry 11.2 ± 3.6, and by Tonopen 13.2 ± 4.1. In the nDSAEK group, mean pressure measured by GAT was 15.0 ± 3.2 mmHg, by DCT 14.4 ± 2.5, by pneumatonometry 12.5 ± 3.2, and by Tonopen 14.4 ± 3.0.

Two-sided paired-difference t tests and Bland-Altman plots indicated that pressure measured by pneumatonometry was significantly and consistently lower than that obtained with the other three methods: GAT (DSAEK, $P < 0.001$; nDSAEK, $P < 0.001$), Tonopen (DSAEK, $P = 0.003$; nDSAEK, $P = 0.003$), and DCT (DSAEK, $P < 0.001$; nDSAEK, $P < 0.001$). This was true in both the DSAEK and nDSAEK groups (Figs. 1, 2).

In the DSAEK group, correlations between pressure and CCT (629 ± 86 μm; mean, 627 μm; range, 482–784 μm) were not statistically significant for any of the techniques: GAT ($r = 0.371$, $P = 0.262$), DCT ($r = 0.353$, $P = 0.287$), pneumatonometry ($r = 0.359$, $P = 0.278$), and Tonopen ($r = 0.107$, $P = 0.754$). The same insignificant findings were true for the nDSAEK group (CCT: 654 ± 40 μm; mean, 660 μm; range,

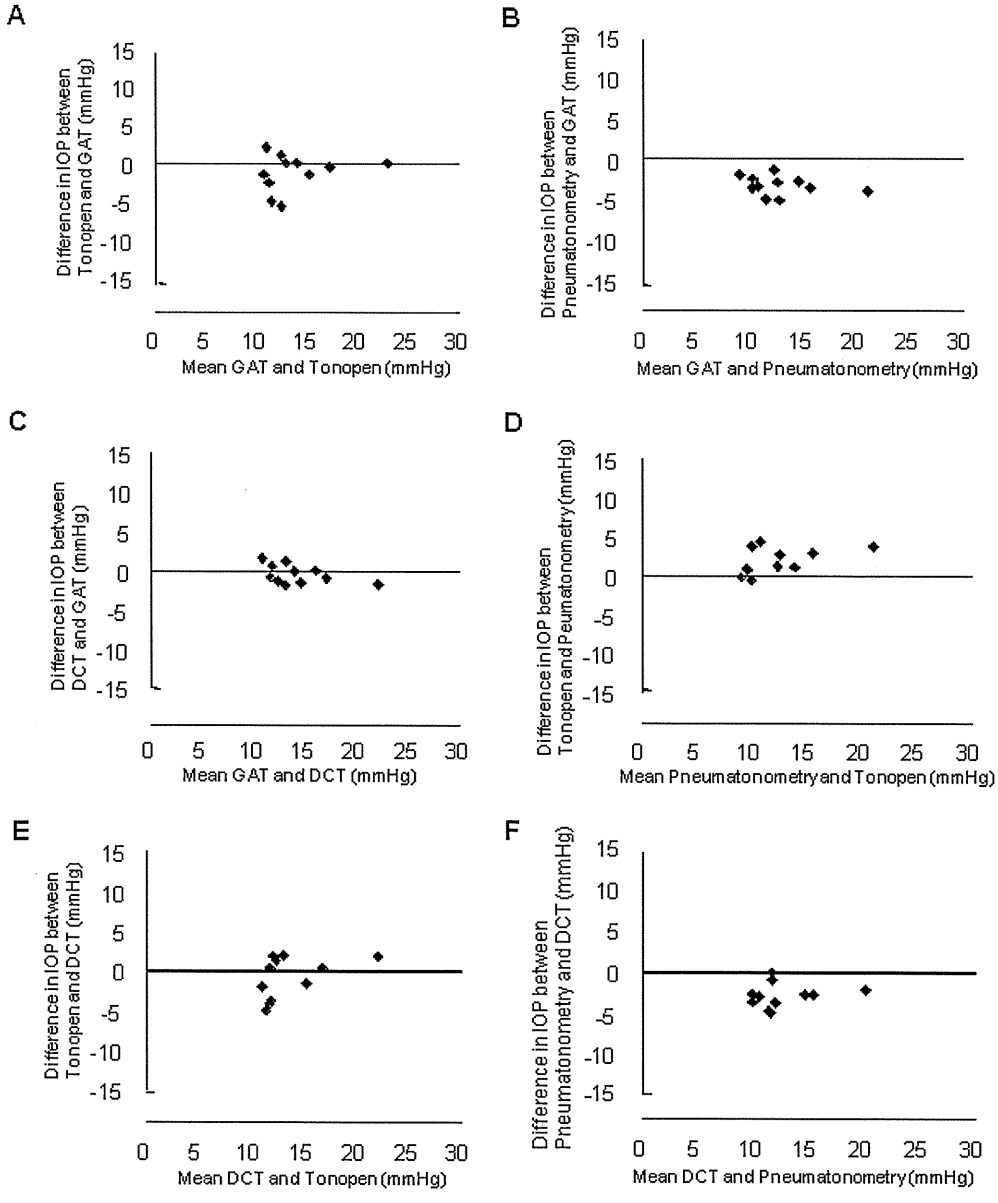

Figure 1A–F. Bland-Altman plots showing means of intraocular pressure (*IOP*) post-DSAEK as measured by two methods plotted against the difference in pressure measured by the same two methods. **A** GAT versus Tonopen (mean difference ± SD = –1.2 ± 2.4 mmHg; P = 0.113). **B** GAT versus pneumatonometry (mean difference ± SD = –3.2 ± 1.2 mmHg; $P < 0.001$). **C** GAT versus DCT (mean difference ± SD = –0.5 ± 1.2 mmHg, $P = 0.235$). **D** Pneumatonometry versus Tonopen (mean difference ± SD = 2.0 ± 1.7 mmHg; P = 0.003). **E** DCT versus Tonopen (mean difference ± SD = –0.8 ± 2.6 mmHg; $P = 0.337$). **F** DCT versus pneumatonometry (mean difference ± SD = –2.8 ± 1.4 mmHg; $P < 0.001$). Three pairs of measurement techniques (GAT versus pneumatonometry, pneumatonometry versus Tonopen, and DCT versus pneumatonometry) were significantly correlated. The remaining pairs (GAT versus Tonopen, GAT versus DCT, DCT versus Tonopen) were not statistically correlated. DSAEK, Descemet's stripping automated endothelial keratoplasty; *GAT*, Goldmann applanation tonometry; *DCT*, dynamic contour tonometry; *Tonopen*, Tono-Pen XL.

584–719 μm): GAT ($r = -0.169$, $P = 0.581$), DCT ($r = -0.272$, P = 0.369), pneumatonometry (r = 0.036, P = 0.906), and Tonopen ($r = -0.016$, $P = 0.959$).

Discussion

After DSAEK surgery, the cornea is significantly thicker than normal because of the microkeratome-dissected donor endothelial lamella, an approximately 100- to 200-μm-thick component of posterior stromal tissue, Descemet's membrane, and endothelium, all attached to the recipient's posterior corneal surface. Recently, successful elimination of the Descemet's membrane stripping process was documented for non-Fuchs-type bullous keratopathy (e.g., aniridia[15] and failed penetrating graft[16]). This procedure is termed nDSAEK,[7,8] and it has produced good clinical outcomes marked by superior visual acuity and minimal induced astigmatism for patients with argon laser iridotomy-induced bullous keratopathies.

Previously, researchers were unable to demonstrate correlations between CCT and IOP as measured by three techniques (GAT, pneumatonometry, and DCT) in DSAEK-treated eyes,[14] indicating that falsely elevated GAT readings, as expected for thick corneas, did not occur after DSAEK treatment. Similarly, in this study we did not find any correlation between CCT and IOP as measured by four different techniques in either the DSAEK or nDSAEK group, a result consistent with previous findings.[14] Taken together, these findings strongly suggest that high IOP readings by GAT, pneumatonometry, DCT, or Tonopen should raise a suspicion of an actually elevated pressure not only

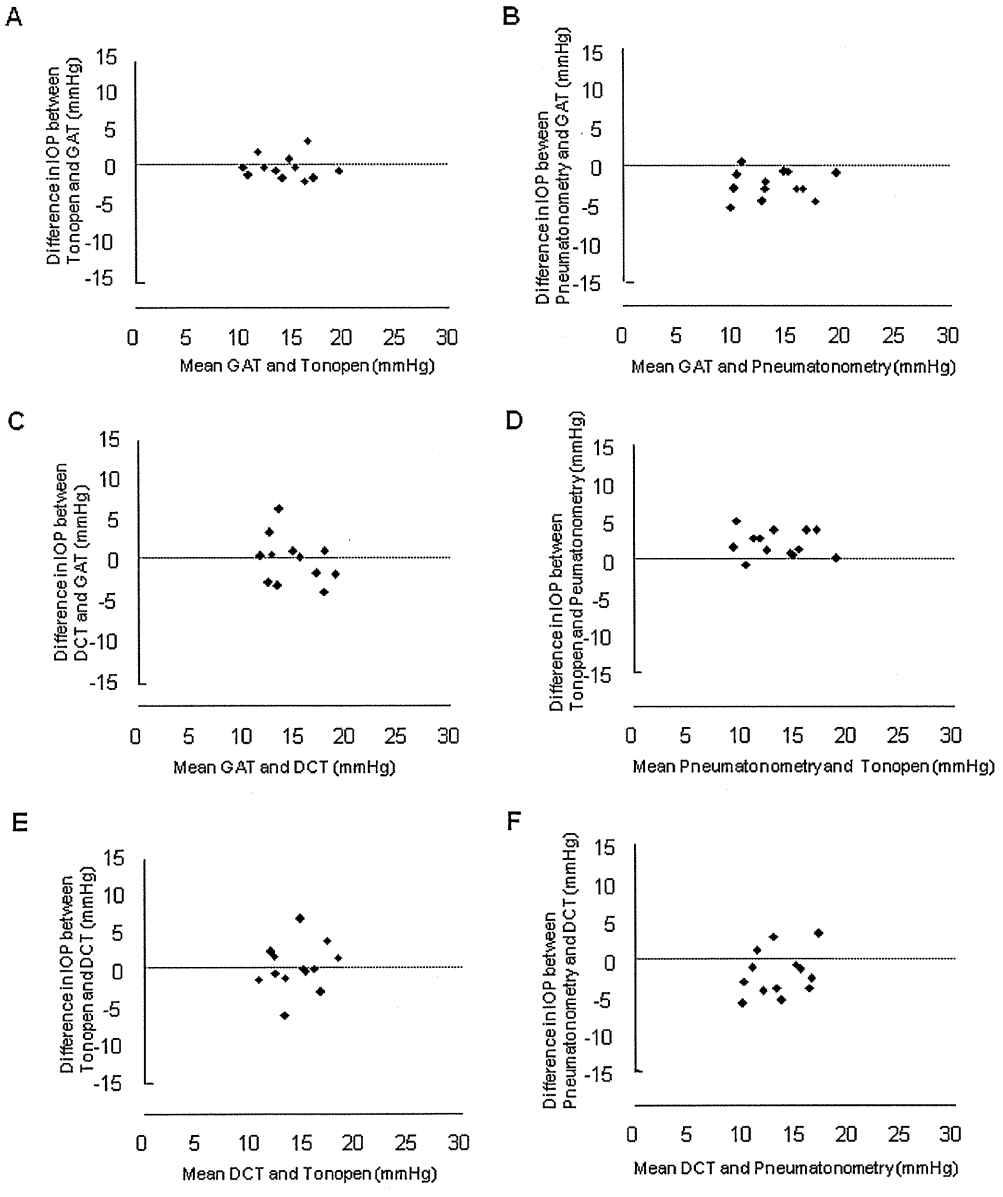

Figure 2A–F. Bland-Altman plots showing means of IOP post-nDSAEK as measured by two methods plotted against the difference in pressure measured by the same two methods. **A** GAT versus Tonopen (mean difference ± SD = –0.6 ± 1.5 mmHg; P = 0.188). **B** GAT versus pneumatonometry (mean difference ± SD = –2.5 ± 1.8 mmHg; $P < 0.001$). **C** GAT versus DCT (mean difference ± SD = –0.6 ± 2.9 mmHg; P = 0.504). **D** Pneumatonometry versus Tonopen (mean difference ± SD = 2.0 ± 1.7 mmHg; $P = 0.002$). **E** DCT versus Tonopen (mean difference ± SD = –0.0 ± 3.0 mmHg; $P = 0.980$). **F** DCT versus pneumatonometry (mean difference ± SD = –2.0 ± 3.0 mmHg; (P = 0.032). Three pairs of measurement techniques (GAT versus pneumatonometry, pneumatonometry versus Tonopen, and DCT versus pneumatonometry) were significantly correlated. The remaining pairs (GAT versus Tonopen, GAT versus DCT, DCT versus Tonopen) were not statistically correlated. nDSAEK, non-Descemet's stripping automated endothelial keratoplasty.

in DSAEK-treated eyes but also in nDSAEK-treated eyes. In other words, both DSAEK-treated and nDSAEK-treated thick corneas behave like normal corneas. Probably, the attached endothelial lamella on the posterior surface of the recipient cornea has little or no effect on the biomechanical properties of the preexisting cornea.

In this study, we showed that pressure measured by pneumatonometry was statistically lower than pressure measured with other techniques (GAT, DCT, and Tonopen); this finding was documented for both DSAEK- and nDSAEK-treated eyes (Figs. 1, 2). In contrast, there was no significant difference between GAT and DCT readings. Recently, Vajaranant and coworkers[14] investigated IOP after DSAEK treatment using three different techniques: GAT, pneumatonometry, and DCT. They reported that, unlike our results, pressure measurements by pneumatonometry and DCT were significantly higher than those obtained with GAT.[14] Previous studies have indicated that pressure readings obtained with DCT are higher than those obtained with GAT, with a range of 0.7–4.4 mmHg in eyes with normal corneas.[17–25] Also, one study reported that pneumatonometry measurements in study subjects treated with laser in situ keratomileusis (LASIK) were approximately 2 mmHg higher than those obtained with GAT.[26] We are unsure why our pressure readings obtained with pneumatonometry were lower than those obtained with the other techniques, or why DCT readings were not higher than the GAT readings. One possible reason is that the low number of patients in this study affected the statistical outcome. Another possible reason is that the presence of host Descemet's membrane or compressed host endothelium plays a role in the results obtained by pressure

measurements with pneumatonometry or DCT. Furthermore, the thinner mean CCT in our study (DSAEK, 629 ± 86 μm; nDSAEK, 654 ± 40 μm) compared with thicknesses reported by Vajaranant and coworkers (701 ± 68 μm)[14] might have influenced readings obtained with either pneumatonometry or DCT or both.

In conclusion, in both DSAEK- and nDSAEK-treated eyes, IOP readings by all four techniques (GAT, DCT, pneumatonometry, and Tonopen) might be independent of artificially enhanced corneal thickness in this small study. Further investigations using a larger number of patients are required to fully elucidate the relationship between intraocular pressure readings and treatment with DSAEK or nDSAEK.

References

1. Melles GR, Eggink FA, Lander F, et al. A surgical technique for posterior lamellar keratoplasty. Cornea 1998;17:618–626.
2. Terry MA, Ousley PJ. Small-incision deep lamellar endothelial keratoplasty (DLEK): six-month results in the first prospective clinical study. Cornea 2005;24:59–65.
3. Terry MA, Ousley PJ. Deep lamellar endothelial keratoplasty: visual acuity, astigmatism, and endothelial survival in a large prospective series. Ophthalmology 2005;112:1541–1548.
4. Price MO, Price FW Jr. Descemet's stripping with endothelial keratoplasty: comparative outcomes with microkeratome-dissected and manually dissected donor tissue. Ophthalmology 2006;113: 1936–1942.
5. Price FW Jr, Price MO. Descemet's stripping with endothelial keratoplasty in 200 eyes: early challenges and techniques to enhance donor adherence. J Cataract Refract Surg 2006;32:411–418.
6. Gorovoy MS. Descemet-stripping automated endothelial keratoplasty. Cornea 2006;25:886–889.
7. Kobayashi A, Yokogawa H, Sugiyama K. Non-Descemet stripping automated endothelial keratoplasty for endothelial dysfunction secondary to argon laser iridotomy. Am J Ophthalmol 2008;146: 543–549.
8. Kobayashi A, Yokogawa H, Sugiyama K. In vivo laser confocal microscopy findings after non-Descemet stripping automated endothelial keratoplasty. Ophthalmology 2009;116:1306–1313.
9. Miyake K, Matsuda M, Inaba M. Corneal endothelial changes in pseudoexfoliation syndrome. Am J Ophthalmol 1989;108:49–52.
10. Kobayashi A, Mawatari Y, Yokogawa H, Sugiyama K. In vivo laser confocal microscopy after Descemet's stripping with automated endothelial keratoplasty. Am J Ophthalmol 2008;145:977–985.
11. Punjabi OS, Kniestedt C, Stamper RL, Lin SC. Dynamic contour tonometry: principle and use. Clin Experiment Ophthalmol 2006;34:837–840.
12. Herndon LW. Measuring intraocular pressure-adjustments for corneal thickness and new technologies. Curr Opin Ophthalmol 2006;17:115–119.
13. Bland JM, Altman DG. Statistical methods for assessing agreement between two methods of clinical measurement. Lancet 1986;1: 307–310.
14. Vajaranant TS, Price MO, Price FW, et al. Intraocular pressure measurements following Descemet stripping endothelial keratoplasty. Am J Ophthalmol 2008;145:780–786.
15. Price MO, Price FW Jr, Trespalacios R. Endothelial keratoplasty technique for aniridic aphakic eyes. J Cataract Refract Surg 2007;33:376–379.
16. Price FW Jr, Price MO. Endothelial keratoplasty to restore clarity to a failed penetrating graft. Cornea 2006;25:895–899.
17. Schneider E, Grehn F. Intraocular pressure measurement—comparison of dynamic contour tonometry and Goldmann applanation tonometry. J Glaucoma 2006;15:2–6.
18. Herdener S, Pache M, Lautebach S, Funk J. Dynamic contour tonometry versus Goldmann applanation tonometry—a comparison of agreement and reproducibility. Graefes Arch Clin Exp Ophthalmol 2007;245:1027–1030.
19. Doyle A, Lachkar Y. Comparison of dynamic contour tonometry with Goldmann applanation tonometry over a wider range of central corneal thickness. J Glaucoma 2005;14:288–292.
20. Francis BA, Hsieh A, Lai M, et al. Effects of corneal thickness, corneal curvature, and intraocular pressure level on Goldmann applanation tonometry and dynamic contour tonometry. Ophthalmology 2007;114:20–26.
21. Martinez JM, Garcia-Feijoo J, Vico E, et al. Effect of corneal thickness on dynamic contour, rebound, and Goldmann tonometry. Ophthalmology 2006;113:2156–2162.
22. Barleon L, Hoffman EM, Berres M, et al. Comparison of dynamic contour tonometry and Goldmann applanation in glaucoma patients and healthy subjects. Am J Ophthalmol 2006;142: 583–590.
23. Kniestedt C, Lin S, Choe J, et al. Clinical comparison of contour and applanation tonometry and their relationship to pachymetry. Arch Ophthalmol 2005;123:1532–1537.
24. Medeiros FA, Sample PA, Weinreb RN. Comparison of dynamic contour tonometry and Goldmann applanation tonometry in African-American subjects. Ophthalmology 2007;114:658–665.
25. Salvetat ML, Zeppieri M, Tosoni C, Brusini P. Comparisons between PASCAL dynamic tonometry, the tonopen, and Goldmann applanation tonometry in patients with glaucoma. Acta Ophthalmol Scand 2007;85:272–279.
26. Zadok D, Tran D, Twa M, et al. Pneumotonometric versus Goldmann tonometry after laser in situ keratomileusis for myopia. J Cataract Refract Surg 1999;25:1344–1348.

Hormonal Regulation of Na^+/K^+-Dependent ATPase Activity and Pump Function in Corneal Endothelial Cells

Shin Hatou, MD†*

Abstract: Na^+- and K^+-dependent ATPase (Na,K-ATPase) in the basolateral membrane of corneal endothelial cells plays an important role in the pump function of the corneal endothelium. We investigated the role of dexamethasone in the regulation of Na,K-ATPase activity and pump function in these cells. Mouse corneal endothelial cells were exposed to dexamethasone or insulin. ATPase activity was evaluated by spectrophotometric measurement, and pump function was measured using an Ussing chamber. Western blotting and immunocytochemistry were performed to measure the expression of the Na,K-ATPase α1-subunit. Dexamethasone increased Na,K-ATPase activity and the pump function of endothelial cells. Western blot analysis indicated that dexamethasone increased the expression of the Na,K-ATPase α_1-subunit but decreased the ratio of active to inactive Na,K-ATPase α_1-subunit. Insulin increased Na,K-ATPase activity and pump function of cultured corneal endothelial cells. These effects were transient and blocked by protein kinase C inhibitors and inhibitors of protein phosphatases 1 (PP1) and 2A (PP2A). Western blot analysis indicated that insulin decreased the amount of inactive Na,K-ATPase α_1-subunit, but the expression of total Na,K-ATPase α_1-subunit was unchanged. Immunocytochemistry showed that insulin increased cell surface expression of the Na,K-ATPase α_1-subunit. Our results suggest that dexamethasone and insulin stimulate Na,K-ATPase activity in mouse corneal endothelial cells. The effect of dexamethasone activation in these cells was mediated by Na,K-ATPase synthesis and an increased enzymatic activity because of dephosphorylation of Na,K-ATPase α_1-subunits. The effect of insulin is mediated by the protein kinase C, PP1, and/or PP2A pathways.

Key Words: corneal endothelium, insulin, ouabain, protein kinase C, protein phosphatase, Na^+- and K^+-dependent ATPase

(*Cornea* 2011;30(Suppl. 1):S60–S66)

A single layer of endothelial cells in a well-arranged mosaic pattern covers the posterior surface of the Descemet membrane in the cornea.[1] Corneal hydration is primarily determined by the balance between penetration of the aqueous humor across the corneal endothelium into the stroma and subsequent pumping of the fluid out of the stroma. The accumulation of fluid in the stroma resulting from disturbance of this balance may lead to bullous keratopathy, which is characterized by an edematous cornea with reduced transparency.[2]

Total pumping activity for the removal of fluid from the cornea is determined by the number of endothelial cells and the pump function of each cell. Given that human corneal endothelial cells have a limited proliferative capacity, endothelial dystrophies, ocular trauma, corneal graft rejection, and insults associated with intraocular surgeries may result in corneal endothelial cell loss and permanent damage. Replacement of the corneal endothelium by keratoplasty is currently the only established therapeutic approach for recovery of endothelial cell number. Pseudophakic or aphakic bullous keratopathy, Fuchs endothelial dystrophy, and failed corneal grafts remain common indications for keratoplasty, accounting for approximately 60% of the total number of such procedures.[3–5] Activation of the pump function in the remaining endothelial cells is a potential alternative approach to recovery of the total pumping activity in the cornea, so long as the total number of such cells is within an acceptable range. However, therapeutic approaches to the activation of corneal endothelial cells remain to be established.

The Na^+- and K^+-dependent ATPase (Na,K-ATPase) expressed in the basolateral membrane of corneal endothelial cells is primarily responsible for the pump function of the corneal endothelium.[1] The Na,K-ATPase pump site density in the corneal endothelium was found to be increased in eyes affected by moderate guttata.[6] Na,K-ATPase pump site density showed an initial increase, a sudden marked decrease, and a subsequent gradual decline associated with the end stage of disease in patients with Fuchs endothelial dystrophy.[7] These observations indicate that certain conditions can induce a compensatory increase in Na,K-ATPase pump site density and, presumably, in endothelial pump function. They also suggest the existence of a regulatory mechanism, or mechanisms, for the control of total Na,K-ATPase activity in the corneal endothelium.

Several studies have shown that glucocorticoids stimulate Na,K-ATPase activity through multiple complex mechanisms, including gene expression, transcription, translocation, and enzymatic activity, in a variety of tissues.[8] Although the results of experimental studies concerning the effects of glucocorticoids on corneal endothelial damage do not show any close correlations,[9–11] topical glucocorticoids have been clinically used for the treatment of corneal

From the *Division for Vision Research, National Institute of Sensory Organs, National Tokyo Medical Center, Tokyo, Japan; and †Department of Ophthalmology, Keio University School of Medicine, Tokyo, Japan.

Supported in part by a grant from the Ministry of Health, Labour and Welfare (Japan).

The author has no financial or conflicts of interest to disclose.

Reprints: Shin Hatou, Department of Ophthalmology, Keio University School of Medicine, 35 Shinanomachi, Shinjuku-ku, Tokyo 160-8582, Japan (e-mail: tr97469@zc4.so-net.ne.jp).

endothelial disorders. Indeed, steroid administration seemed to increase endothelial pump function and ameliorate stromal edema in a patient with bullous keratopathy secondary to Sato refractive surgery.[12] In contrast, clinical observations of a higher incidence of persistent corneal edema after vitrectomy and other surgical procedures for patients with diabetes mellitus have suggested that abnormal corneal endothelial function is associated with diabetes mellitus.[13–18] Specular microscopic studies have shown morphological abnormalities, such as lower endothelial cell density and increased endothelial pleomorphism, in patients with types 1 and 2 diabetes mellitus.[18–27] Some clinical studies have shown that diabetic patients tend to have slightly thicker corneas and a reduced recovery rate from hypoxia-induced corneal edema.[28–31] These observations led us to the idea that Na,K-ATPase activity and pump function of the corneal endothelium may be affected by several hormones, such as glucocorticoids or insulin.

In this review, we outline methods for measuring the enzymatic activity and pump function of Na,K-ATPase in cultured mouse corneal endothelial cells. This is followed by a review of the roles of dexamethasone and insulin in controlling the enzymatic activity and pump function of Na,K-ATPase in corneal endothelial cells. Additionally, we present the mechanisms by which dexamethasone or insulin might affect Na,K-ATPase activity.

MEASUREMENT OF Na,K-ATPase ENZYME ACTIVITY

Corneal endothelial cells were cultured with or without dexamethasone, insulin, staurosporine, GF109203X, or okadaic acid. To measure Na,K-ATPase enzyme activity, ouabain (final concentration, 1 mM) or vehicle was added to cell cultures and incubated for 30 minutes at 37°C. After further addition of adenosine triphosphate (final concentration, 10 mM), the adenosine triphosphate hydrolysis reaction catalyzed by Na,K-ATPase released phosphate. The concentration of phosphate was determined by spectrophotometric measurement with ammonium molybdate. The Na,K-ATPase activity was calculated as the difference in phosphate concentration between cells with and without ouabain.

MEASUREMENT OF ELECTRICAL Na,K-ATPase PUMP FUNCTION

To measure pump function, cells cultured on Snapwell inserts were placed in an Ussing chamber. The endothelial cell surface side was in contact with 1 chamber and the Snapwell membrane side was in contact with another chamber. If Na,K-ATPase was active, then a short-circuit current would be evoked by active sodium and potassium flux. After the short-circuit current had reached a steady state, ouabain was added. The pump function attributable to Na,K-ATPase activity was calculated as the difference in short-circuit current measured before and after the addition of ouabain (Fig. 1).

DEXAMETHASONE STIMULATES Na,K-ATPase ACTIVITY

Mouse corneal endothelial cells were exposed to 10 μM dexamethasone for various periods and Na,K-ATPase activity was then measured. Dexamethasone increased Na,K-ATPase activity in a time-dependent manner, with this effect being significant ($P < 0.05$; Student t test) at 6 hours and maximal at 48 hours (Fig. 2). The stimulatory effect of dexamethasone on Na,K-ATPase activity was also concentration dependent (Fig. 2).[32] The stimulatory effect of dexamethasone on pump function was time dependent, being significant at 24 hours and maximal at 48 hours (Fig. 3A),[32] and concentration dependent, which was apparent at 1 or 10 μM (Fig. 3B).[32] These results were similar to those obtained for Na,K-ATPase activity.

To determine whether dexamethasone affects Na,K-ATPase expression in corneal endothelial cells, we exposed the cells to dexamethasone for 48 hours and measured the expression of total Na,K-ATPase α_1-subunit and phospho-Na,K-ATPase α_1-subunit by Western blot analysis. Phospho-Na,K-ATPase α_1-subunit is considered to be the inactive state of the Na,K-ATPase α_1-subunit. Levels of the Na,K-ATPase α_1-subunit and phospho-Na,K-ATPase α_1-subunit were measured and are presented as relative amounts compared with the signal intensities for β-actin (Fig. 4A).[32] Dexamethasone increased the expression of total Na,K-ATPase α_1-subunit in a concentration-dependent manner, whereas it did not alter the expression of the phospho-Na,K-ATPase α_1-subunit (Figs. 4B, C)[32]; therefore, the ratio of phospho-Na,K-ATPase α_1-subunit expression to total Na,K-ATPase α_1-subunit expression was decreased in a concentration-dependent manner (Fig. 4D).[32]

INSULIN TRANSIENTLY ACTIVATES Na,K-ATPase

To determine whether insulin affects Na,K-ATPase activity in corneal endothelial cells, we exposed the cells to 0.1 μM insulin for various periods and measured the

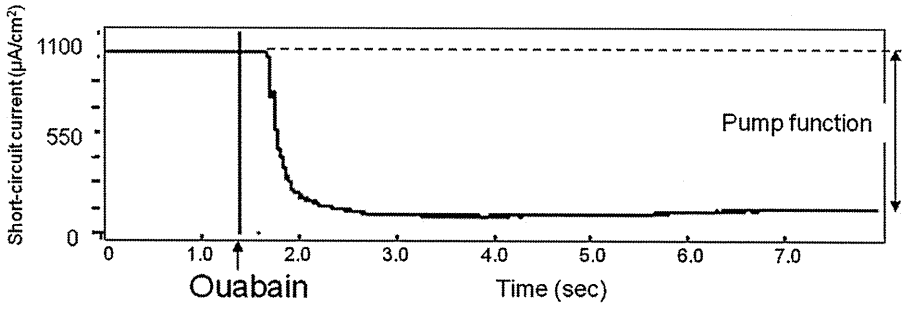

FIGURE 1. Representative trace of short-circuit current (microamperes per well) obtained with cell monolayers in an Ussing chamber. The insert well membrane growth area was 4.67 cm^2. Pump function attributable to Na,K-ATPase activity was calculated as the difference in short-circuit currents obtained before and after the addition of ouabain.

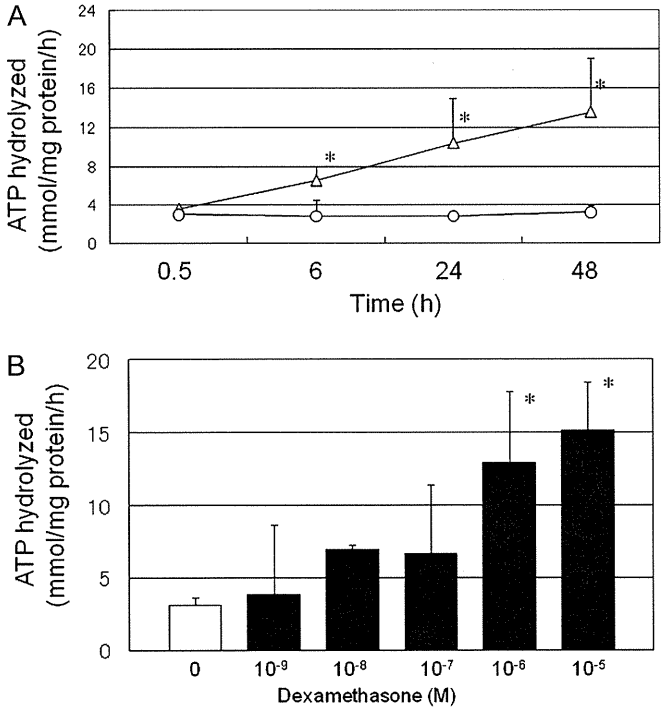

FIGURE 2. Effect of dexamethasone on Na,K-ATPase activity in cultured mouse corneal endothelial cells. A, Cells were incubated in the absence (circles) or presence (triangles) of 10 μM dexamethasone for the indicated times and then assayed for Na,K-ATPase activity. *$P < 0.05$ versus the corresponding value for cells incubated without dexamethasone (Student t test). B, Cells were incubated with the indicated concentrations of dexamethasone for 48 hours and then assayed for Na,K-ATPase activity. *$P < 0.01$ for the indicated comparisons (Student t test). Modified with permission from Hatou et al.[32]

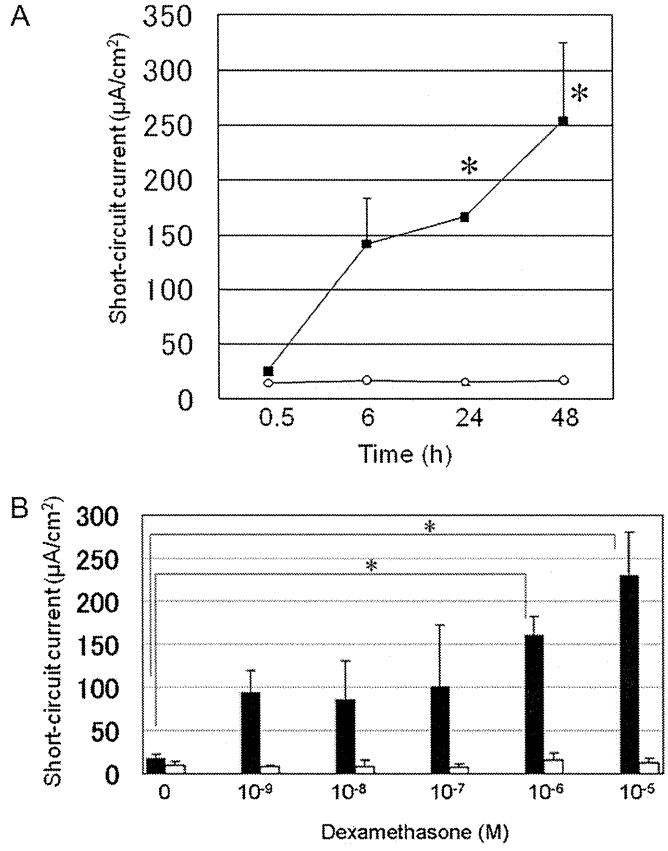

FIGURE 3. Effect of dexamethasone on the pump function of cultured mouse corneal endothelial cells. A, Cells were incubated in the absence (circles) or presence (squares) of 10 μM dexamethasone for the indicated times and then assayed for pump function (microamperes per square centimeter). *$P < 0.05$ versus the corresponding value for cells incubated without dexamethasone (Student t test). (B) Pump function (microamperes per square centimeter) attributable to Na,K-ATPase activity was determined 48 hours after incubation of cells in the presence of the indicated concentrations of dexamethasone (black). Ouabain-independent short-circuit current (white) is also presented, which did not change significantly with the indicated concentrations of dexamethasone. Data are means ± SDs of values from 4 replicate experiments. *$P < 0.05$ for the indicated comparisons (Student t test). Modified with permission from Hatou et al.[32]

Na,K-ATPase activity. Insulin had a transient stimulatory effect on Na,K-ATPase activity, with this effect being significant at 6 and 12 hours. After 12 hours, Na,K-ATPase activity returned to baseline levels. The stimulatory effect of insulin on Na,K-ATPase activity was also concentration dependent (Fig. 5).[33]

We next examined whether insulin affects the pump function of corneal endothelial cells. Insulin at 0.1 μM increased the ouabain-sensitive pump function of the corneal endothelial cells compared with control cells. This effect of insulin was statistically significant ($P < 0.05$) at 6 hours. The stimulatory effect of insulin on pump function was concentration dependent, and these results were similar to the results obtained for Na,K-ATPase activity (Fig. 6).[33]

PROTEIN KINASE C MEDIATION OF INSULIN-INDUCED Na,K-ATPase ACTIVATION

To test whether the stimulatory effect of insulin on Na,K-ATPase activity was mediated by protein kinase C (PKC), we examined the effects of staurosporine and GF109203X. The increase in Na,K-ATPase activity induced by insulin was significantly inhibited ($P < 0.01$) by staurosporine and GF109203X (Fig. 7).[33] We next examined whether okadaic acid affected the Na,K-ATPase activation induced by insulin. The activity of Na,K-ATPase in conjunction with 0.1 μM insulin was significantly reduced ($P < 0.01$) in the presence of 1 μM okadaic acid (Fig. 7).[33]

We exposed cells to 0.1 μM insulin for 6 hours and then measured the expression levels of total Na,K-ATPase α_1-subunit and phospho-Na,K-ATPase α_1-subunit by Western blotting to determine whether insulin affected Na,K-ATPase expression in corneal endothelial cells. Although there was no statistically significant difference in the expression of total Na,K-ATPase α_1-subunit (Fig. 8A, B),[33] insulin significantly decreased ($P < 0.05$) the ratio of phospho-Na,K-ATPase α_1-subunit expression to total Na,K-ATPase α_1-subunit (Fig. 8C).[33]

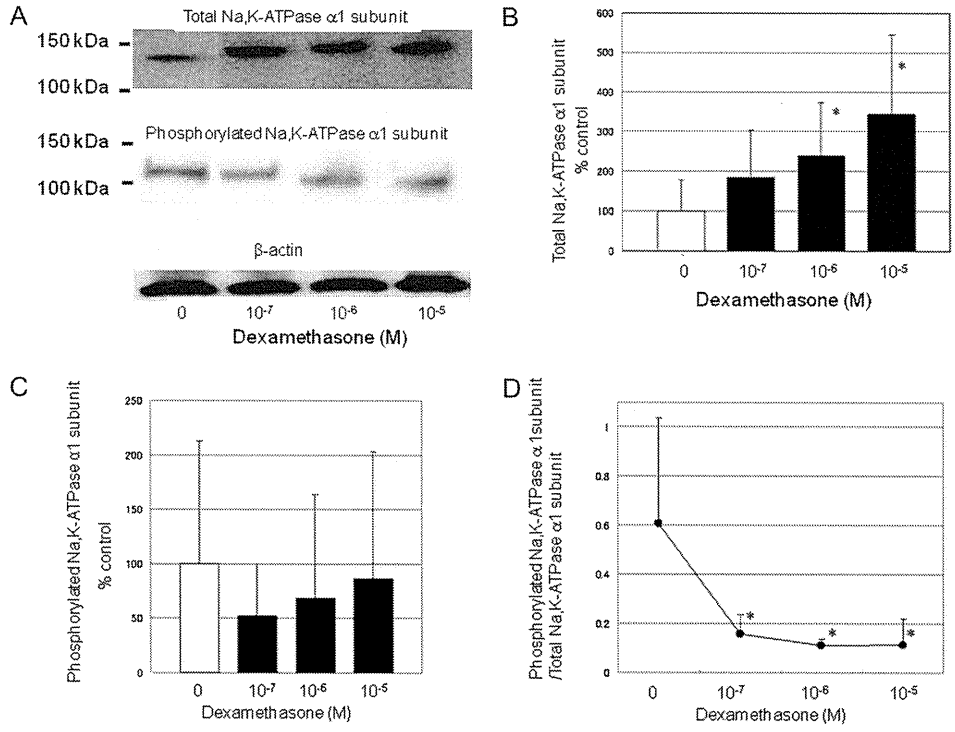

FIGURE 4. Western blot analysis of Na,K-ATPase α_1-subunit and phospho-Na,K-ATPase α_1-subunit expression. A, Representative signals of expression. Top: Na,K-ATPase α_1-subunit. Middle: phospho-Na,K-ATPase α_1-subunit. Bottom: β-actin. The relative intensity of each band with respect to β-actin was measured and expressed as a ratio. B, Cells were incubated with the indicated concentrations of dexamethasone for 48 hours and then assayed for expression of the Na,K-ATPase α_1-subunit. Data are means ± SDs from 5 experiments, expressed as a percentage of control. $*P < 0.05$ for the indicated comparisons (Student *t* test). C, Cells were incubated with the indicated concentrations of dexamethasone for 48 hours and then assayed for expression of the phospho-Na,K-ATPase α_1-subunit. Data are means ± SDs from 5 experiments, expressed as a percentage of control. D, The rate of the inactive state of Na,K-ATPase α_1-subunit with the indicated concentrations of dexamethasone. The values represent the ratio of phospho-Na,K-ATPase α_1-subunit expression to Na,K-ATPase α_1-subunit expression. Data are means ± SDs of values from 5 experiments. $*P < 0.05$ for the indicated comparisons (Student *t* test). Modified with permission from Hatou et al.[32]

In the presence of staurosporine, GF109203X, and okadaic acid, the expression of total Na,K-ATPase α_1-subunit was unchanged; however, insulin-induced dephosphorylation of the Na,K-ATPase α_1-subunit was diminished.

Immunocytochemistry was employed to determine whether the effects of insulin changed cell surface expression of the Na,K-ATPase α_1-subunit. Insulin-treated corneal endothelial cells expressed more Na,K-ATPase α_1-subunit at their lateral cell membranes compared with control cells. In the presence of inhibitors, such as GF109203X, Na,K-ATPase α_1-subunit expression at the lateral cell membrane was observed to be decreased (Fig. 9A–C).[33]

DISCUSSION

We have shown that dexamethasone increases Na,K-ATPase activity and pump function in cultured corneal endothelial cells. Changes in Na,K-ATPase activity and pump function were strongly correlated under various experimental conditions. Our results support the stimulatory effect of dexamethasone on Na,K-ATPase activity in corneal endothelial cells.

Our results further suggest that the regulation of Na,K-ATPase activity by dexamethasone in corneal endothelial cells was mediated by Na,K-ATPase subunit synthesis. Na,K-ATPase is the largest protein complex in the family of P-type cation pumps, and its minimum functional unit is a heterodimer of the α- and β-subunits.[34] Ewart and Klip[8] reported that the activation of Na,K-ATPase by steroid hormones seemed to be mediated by the synthesis of new α- and β-subunits. In our study, dexamethasone increased the proportion of active-state Na,K-ATPase α_1-subunits and the total number of Na,K-ATPase α_1-subunits. The antiphospho-Na/K-ATPase α_1 antibody we used recognizes the Na,K-ATPase α_1-subunit only when phosphorylated at Ser-18. Phosphorylation at Ser-18 triggers endocytosis of Na,K-ATPase α_1-subunits and results in inhibition of Na,K-ATPase activity.[35,36] Dexamethasone may prevent Na,K-ATPase α_1-subunits from Ser-18 phosphorylation and thereby increase the proportion of active-state Na,K-ATPase α_1-subunits.

Our results showed that insulin increased Na,K-ATPase activity and pump function in cultured corneal endothelial cells, but the observed effect of insulin on Na,K-ATPase activity was transient. A lack of insulin in type 1 diabetes mellitus or a chronic reduced level of insulin signaling because of insulin resistance in type 2 diabetes mellitus is essential for the pathogenesis of corneal abnormalities in diabetes.

Insulin has been shown to stimulate electrogenic sodium transport in a variety of cells.[8,37–46] In most cases, the increase in Na^+ transport is thought to be a result of the stimulation of Na,K-ATPase. There have been various advocated mechanisms of insulin action, including changes in the kinetic properties of the enzyme,[37,38] an increase in the intracellular Na^+ concentration that leads to subsequent pump stimulation,[39–43] and an increase in the pump concentration at the cell surface by serum- and glucocorticoid-dependent kinase.[44–46] Regardless of whether insulin stimulates pump activity by a previous increase in cytosolic Na^+, its affinity for Na^+, or in-pump availability at the cell surface, the insulin receptor

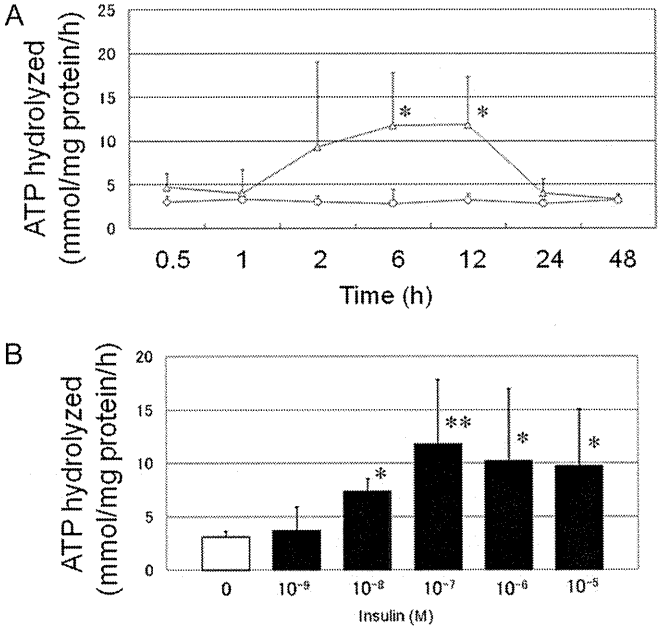

FIGURE 5. Effect of insulin on Na,K-ATPase activity in cultured mouse corneal endothelial cells. A, Cells were incubated in the absence (circles) or presence (triangles) of 0.1 μM insulin for the indicated times and then assayed for Na,K-ATPase activity. Data are means ± SDs of values from 4 replicate experiments. $*P < 0.05$ versus the corresponding value for cells incubated without insulin (Student *t* test). B, Cells were incubated with the indicated concentrations of insulin for 6 hours and then assayed for Na,K-ATPase activity. Data are means ± SDs of values from 4 replicates of 4 representative experiments. $*P < 0.05$, $**P < 0.01$ for the indicated comparisons (Student *t* test). Modified with permission from Hatou et al.[33]

signaling cascades must be involved.[8] These signaling cascades include those mediated by protein kinases, such as PKC. PKC is thought to trigger the rapid action of insulin on Na,K-ATPase and to be involved in the stimulation of Na,K-ATPase by insulin in muscle cells.[8] In our study, Western blot analysis suggested that the stimulation of Na,K-ATPase activity by insulin in corneal endothelial cells was associated with a decrease in the levels of the inactive state of the Na,K-ATPase α_1-subunit. Na,K-ATPase activation by insulin seemed to be mediated by PKC, protein phosphatase 1 (PP1), and/or PP2A. The immunocytochemistry results indicated that insulin increased cell surface expression of the Na,K-ATPase α_1-subunit, and the presence of inhibitors, such as GF109203X, decreased its expression.

In conclusion, we have shown that dexamethasone and insulin increase Na,K-ATPase activity and pump function in corneal endothelial cells. Furthermore, our results support a model in which Na,K-ATPase activation by dexamethasone is mediated by Na,K-ATPase subunit synthesis and an increase in the proportion of Na,K-ATPase α_1-subunits in the active state. In contrast, the observed effect of insulin on Na,K-ATPase activity was transient. This may be because Na,K-ATPase activation by insulin in corneal endothelial cells was mediated by an increase in the active state of the Na,K-ATPase α_1-subunits via PKC, PP1, and/or PP2A pathways, but not by Na,K-ATPase subunit synthesis. A lack of insulin in type 1 diabetes mellitus or a reduced level of insulin signaling caused by insulin resistance in type 2 diabetes mellitus may play a role in the pathogenesis of corneal abnormalities in diabetes. Pharmacological manipulation of dexamethasone or insulin in corneal endothelial cells is a potential therapeutic approach for increasing the pump function in corneal endothelial cells.

REFERENCES

1. Nishida T. Cornea. In: Krachmer JH, Mannis MJ, Holland EJ, eds. *Cornea*. 2nd ed. London, United Kingdom: Elsevier Mosby; 2005:3–26.
2. Feiz V. Corneal edema. In: Krachmer JH, Mannis MJ, Holland EJ, eds. *Cornea*. 2nd ed. London, United Kingdom: Elsevier Mosby; 2005: 359–363.
3. Kang PC, Klintworth GK, Kim T, et al. Trends in the indications for penetrating keratoplasty, 1980–2001. *Cornea*. 2005;24:801–803.
4. Al-Yousuf N, Mavrikakis E, Daya SM. Penetrating keratoplasty: indications over 10 year period. *Br J Ophthalmol*. 2004;88:998–1001.
5. Dobbins KR, Price FW Jr, Whitson WE. Trends in the indications for penetrating keratoplasty in the Midwestern United States. *Cornea*. 2000; 19:813–816.

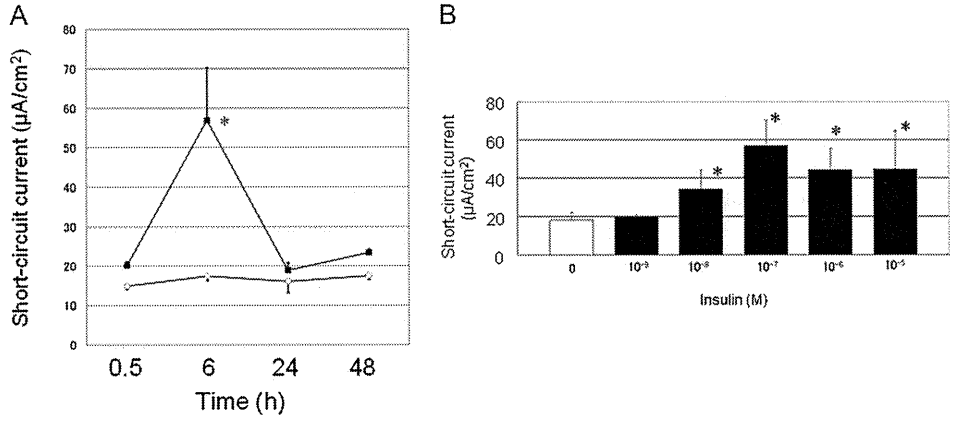

FIGURE 6. Effect of insulin on the pump function of cultured mouse corneal endothelial cells. A, Pump function (microamperes per square centimeter) attributable to Na,K-ATPase activity was determined in the absence (circles) or presence (squares) of 0.1 μM insulin for the indicated times. Data are means ± SDs of values from 4 replicates of a representative experiment. $*P < 0.05$ versus the corresponding value for cells incubated without insulin (Student *t* test). B, Pump function (microamperes per square centimeter) attributable to Na,K-ATPase activity was determined 6 hours after incubation of cells in the presence of the indicated concentrations of insulin. Data are means ± SDs of values from 4 replicates of 4 representative experiments. $*P < 0.05$ for the indicated comparisons (Student *t* test). Modified with permission from Hatou et al.[33]

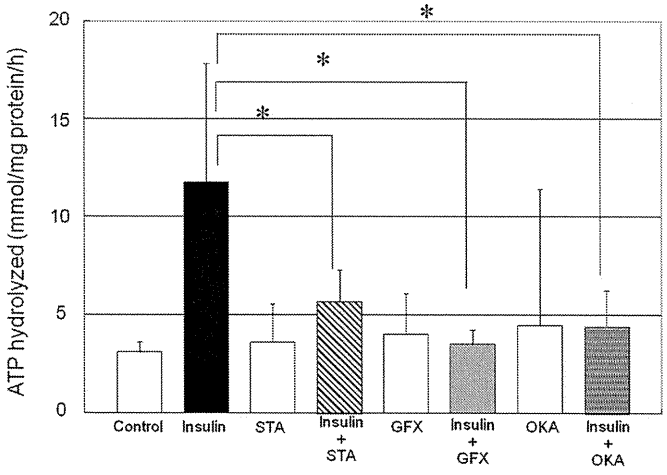

FIGURE 7. Effect of staurosporine (STA), GF109203X (GFX), and okadaic acid (OKA) on insulin-induced Na,K-ATPase activity in cultured mouse corneal endothelial cells. Cells were incubated for 30 minutes in the absence or presence of 1 μM staurosporine, 0.1 μM GF109203X, or 1 μM okadaic acid and then for an additional 6 hours in the presence of 0.1 μM insulin before measurement of Na,K-ATPase activity. Data are means ± SDs of values from 4 replicates of 4 representative experiments. $*P < 0.01$ versus the value for cells incubated with insulin alone (Student *t* test). Na,K-ATPase activity did not significantly increase in the presence of staurosporine + insulin, GF109203X + insulin, or okadaic acid + insulin compared with controls. Modified with permission from Hatou et al.[33]

6. Georski D, Matsuda M, Yee RW, et al. Pump function of the human corneal endothelium. Effects of age and cornea guttata. *Ophthalmology.* 1985;92:759–763.
7. McCartney MD, Wood TO, McLaughlin BJ. Moderate Fuchs' endothelial dystrophy ATPase pump site density. *Invest Ophthalmol Vis Sci.* 1989;30: 1560–1564.
8. Ewart NS, Klip A. Hormonal regulation of the Na^+,K^+-ATPase: mechanisms underlying rapid and sustained changes in pump activity. *Am J Physiol.* 1995;269:C295–C311.
9. Sanchez RO, Polack FM. Effect of topical steroids on the healing of corneal endothelium. *Invest Ophthalmol Vis Sci.* 1974;13:17–22.
10. Chung JH, Paek S, Choi JJ, et al. Effect of topically applied 0.1% dexamethasone on endothelial healing and aqueous composition during the repair process of rabbit corneal alkali wounds. *Curr Eye Res.* 1999;18: 110–116.
11. Olsen E, Dacanger M. The effect of steroids on the healing of the corneal endothelium. An in vivo and in vitro study in rabbits. *Acta Ophthalmol Scand.* 1984;62:893–899.
12. Fukuda K, Takeuchi H, Nishida T. A case of noninflammatory corneal edema following anterior-posterior radial keratotomy (Sato's operation) successfully treated by topical corticosteroid. *Jpn J Ophthalmol.* 2000;44: 520–523.
13. Brightbill FS, Meyers FL, Brensnick GH. Post-vitrectomy keratopathy. *Am J Ophthalmol.* 1978;85:651–655.
14. Foulks GN, Thoft RA, Perry HD, et al. Factors related to corneal epithelial complications after closed vitrectomy in diabetics. *Arch Ophthalmol.* 1979;97:1076–1079.
15. Perry HD, Foulks GN, Thoft RA, et al. Corneal complications after closed vitrectomy through the pars plana. *Arch Ophthalmol.* 1980;96:1401–1403.
16. Mandelcorm MS, Blankenship G, Machemer R. Pars plana vitrectomy for the management of severe diabetic retinopathy. *Am J Ophthalmol.* 1976; 81:561–570.
17. Schultz RO, Van Horn D, Peters MA, et al. Diabetic keratopathy. *Trans Am Ophthalmol Soc.* 1981;79:180–198.

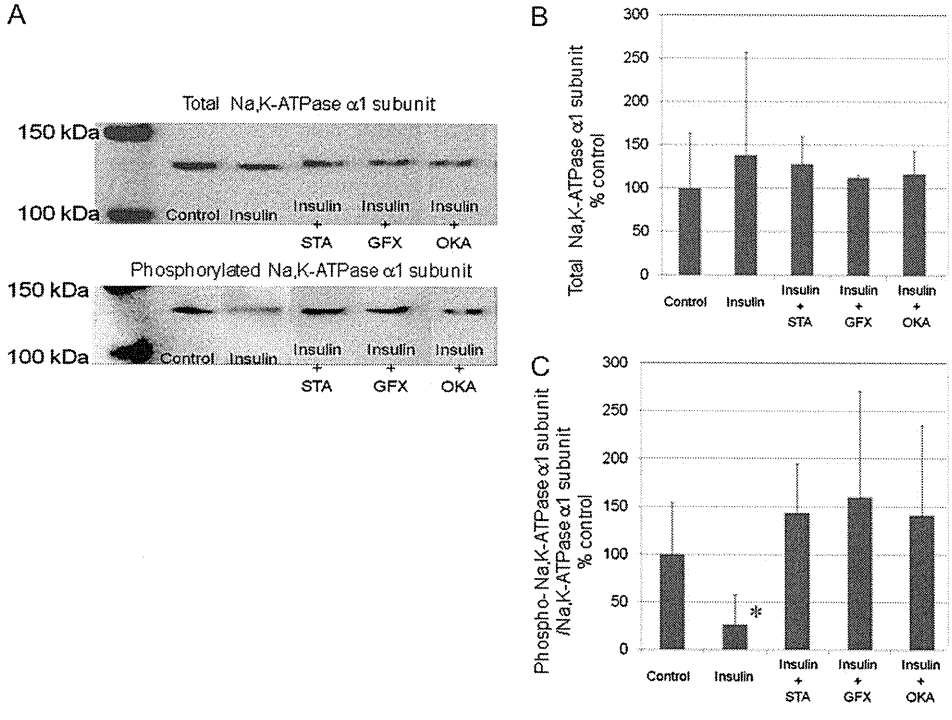

FIGURE 8. Western blot analysis of Na,K-ATPase α_1-subunit and phospho-Na,K-ATPase α_1-subunit expression. A, Representative signals of expression. Top: Na,K-ATPase α_1-subunit. Bottom: phospho-Na,K-ATPase α_1-subunit. The relative intensity of each band compared with β-actin was measured by a densitometer and expressed as a ratio. B, Cells were incubated in the absence (control) or presence of 0.1 μM insulin for 6 hours, 0.1 μM insulin for 6 hours with a 30-minute preincubation with 1 μM staurosporine (insulin + STA), 0.1 μM GF109203X (insulin + GFX), or 1 μM okadaic acid (insulin + OKA) and then assayed for the expression of Na,K-ATPase α_1-subunit. Data are means ± SDs from 5 experiments, expressed as a percentage of control. C, The rate of inactive state of Na,K-ATPase α_1-subunit with insulin, insulin + STA, insulin + GFX, and insulin + OKA. The values represent the ratio of phospho-Na,K-ATPase α_1-subunit expression to Na,K-ATPase α_1-subunit expression. Data are means ± SDs of values from 5 experiments. $*P < 0.05$ versus the value for cells incubated without insulin (Student *t* test). Modified with permission from Hatou et al.[33]

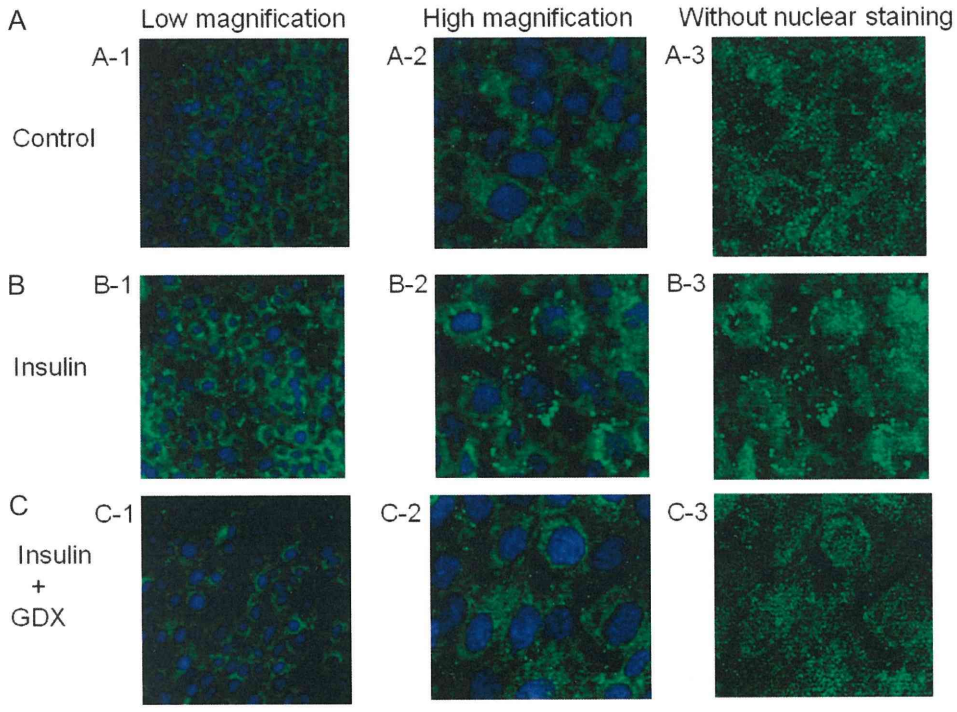

FIGURE 9. Effect of insulin on Na,K-ATPase α_1-subunit cell surface expression. Cells were incubated in the absence of insulin (A) or in the presence of 0.1 μM insulin for 6 hours (B) or 0.1 μM insulin for 6 hours with a 30-minute preincubation with 1 μM GF109203X (C) and then assayed for cell surface expression of the Na,K-ATPase α_1-subunit by immunocytochemistry. A-1, B-1, and C-1: low magnification; A-2, B-2, and C-2: high magnification; and A-3, B-3, and C-3: without nuclear staining. Modified with permission from Hatou et al.[33]

18. Rao GN, Aquavella JV, Goldberg SH, et al. Pseudophakic bullous keratopathy: relationships to preoperative endothelial status. *Ophthalmology.* 1984;91:1135–1140.
19. Rao GN, Shaw EL, Arther EJ, et al. Endothelial cell morphology and corneal deturgescence. *Ann Ophthalmol.* 1978;11:885–899.
20. O'Niel MR, Polse KA. Decreased endothelial pump function with aging. *Invest Ophthalmol Vis Sci.* 1986;27:457–463.
21. Schultz RO, Matsuda M, Yee RW, et al. Corneal endothelial changes in type 1 and type 2 diabetes mellitus. *Am J Ophthalmol.* 1984;98:401–410.
22. Kim EK, Geroski DH, Holley GP, et al. Corneal endothelial cytoskeletal changes in F-actin with aging, diabetes, and after cytochalasin exposure. *Am J Ophthalmol.* 1992;114:331–335.
23. Roszkowska AM, Tringali CG, Colosi P, et al. Corneal endothelium evaluation in type 1 and type 2 diabetes mellitus. *Ophthalmologica.* 1999; 213:258–261.
24. Inoue K, Kato S, Inoue Y, et al. Corneal endothelium and thickness in type 2 diabetes mellitus. *Jpn J Ophthalmol.* 2002;46:65–69.
25. Take G, Karabay G, Erdogan D, et al. The ultrastructural alterations in rat corneas with experimentally-induced diabetes mellitus. *Saudi Med J.* 2006;27:1650–1655.
26. Busted N, Olsen T, Schmitz O. Clinical observations on the corneal thickness and the corneal endothelium in diabetes mellitus. *Br J Ophthalmol.* 1981;65:687–690.
27. Olsen T, Busted N. Corneal thickness in eyes with diabetic and nondiabetic neovascularisation. *Br J Ophthalmol.* 1981;65:691–693.
28. Weston BC, Bourne WM, Polse KA, et al. Corneal hydration control in diabetes mellitus. *Invest Ophthalmol Vis Sci.* 1995;36:586–595.
29. Pierro L, Brancato R, Zaganelli E. Correlation of corneal thickness with blood glucose control in diabetes mellitus. *Acta Ophthalmol (Copenh).* 1993;71:169–172.
30. Skaff A, Cullen AP, Doughty MJ, et al. Corneal swelling and recovery following wear of thick hydrogel contact lenses in insulin-dependent diabetics. *Ophthalmol Physiol Opt.* 1995;15:287–297.
31. Saini JS, Mittal S. In vivo assessment of corneal endothelial function in diabetes mellitus. *Arch Ophthalmol.* 1996;114:649–653.
32. Hatou S, Yamada M, Mochizuki H, et al. The effects of dexamethasone on the Na,K-ATPase activity and pump function of corneal endothelial cells. *Curr Eye Res.* 2009;34:347–354.
33. Hatou S, Yamada M, Akune Y, et al. Role of insulin in regulation of Na+-/K+-dependent ATPase activity and pump function in corneal endothelial cells. *Invest Ophthalmol Vis Sci.* 2010;51:3935–3942.
34. Jorgensen PL, Hakansson KO, Karlish SJ. Structure and mechanism of Na,K-ATPase: functional sites and their interactions. *Annu Rev Physiol.* 2003;65:817–849.
35. Chibalin AV, Ogimoto G, Pedemonte CH, et al. Dopamine-induced endocytosis of Na+,K+-ATPase is initiated by phosphorylation of Ser-18 in the rat alpha subunit and is responsible for the decreased activity in epithelial cells. *J Biol Chem.* 1999;274:1920–1927.
36. Yudowski GA, Efendiev R, Pedemonte CH, et al. Phosphoinositide-3 kinase binds to a proline-rich motif in the Na+, K+-ATPase alpha subunit and regulates its trafficking. *Proc Natl Acad Sci U S A.* 2000;97:6556–6561.
37. Feraille E, Carranza ML, Rousselot M, et al. Insulin enhances sodium sensitivity of Na-K-ATPase in isolated rat proximal convoluted tubule. *Am J Physiol.* 1994;267(pt2):F55–F62.
38. Deachapunya C, Palmer-Densmore M, O'Grady SM. Insulin stimulates transepithelial sodium transport by activation of a protein phosphatase that increases Na-K ATPase activity in endometrial epithelial cells. *J Gen Physiol.* 1999;114:561–574.
39. Siegel B, Civan MM. Aldosterone and insulin effects on driving force of Na^+ pump in toad bladder. *Am J Physiol.* 1976;230:1603–1608.
40. Walker TC, Fidelman ML, Watlington CO, et al. Insulin decreases apical membrane resistance in cultured kidney cells (A6). *Biochem Biophys Res Commun.* 1984;124:614–618.
41. Blazer-Yost BL, Cox M, Furlanetto J. Insulin and IGF-I receptor-mediated Na^+ transport in toad urinary bladders. *Am J Physiol.* 1989;257:C612–C620.
42. McGill DL, Guidotti G. Insulin stimulates both the alpha 1 and the alpha 2 isoforms of the rat adipocyte (Na+,K+) ATPase. Two mechanisms of stimulation. *J Biol Chem.* 1991;266:15824–15831.
43. Erlij D, De Smet P, Van Driessche W. Effect of insulin on area and Na^+ channel density of apical membrane of cultured toad kidney cells. *J Physiol.* 1994;481:533–542.
44. Henke G, Setiawan I, Bohmer C, et al. Activation of Na^+/K^+-ATPase by the serum and glucocorticoid-dependent kinase isoforms. *Kidney Blood Press.* 2002;25:370–374.
45. Park J, Leong ML, Buse P, et al. Serum and glucocorticoid-inducible kinase (SGK) is a target of the PI 3-kinase-stimulated signaling pathway. *EMBO J.* 1999;18:3024–3033.
46. Verry F, Summa V, Heitzmann D, et al. Short-term aldosterone action on Na,K-ATPase surface expression: role of aldosterone-induced SGK1? *Ann N Y Acad Sci.* 2003;986:554–561.

In Vivo Confocal Microscopic Evidence of Keratopathy in Patients with Pseudoexfoliation Syndrome

Xiaodong Zheng,[1] *Atsushi Shiraishi,*[1] *Shinichi Okuma,*[1] *Shiro Mizoue,*[1] *Tomoko Goto,*[1,2] *Shiro Kawasaki,*[1] *Toshihiko Uno,*[1,3] *Tomoko Miyoshi,*[1,2] *Alfredo Ruggeri,*[4] *and Yuichi Ohashi*[1]

Purpose. To measure the density of cells in different layers of the cornea and to determine whether morphologic changes of the subbasal corneal nerve plexus are present in eyes with the pseudoexfoliation (PEX) syndrome.

Methods. Twenty-seven patients with unilateral PEX syndrome and 27 normal controls were investigated. All eyes underwent corneal sensitivity measurements with an esthesiometer and in vivo confocal microscopic study. Densities of the epithelial, stromal, and endothelial cells were measured. The density and tortuosity of the subbasal corneal nerve plexus were also evaluated.

Results. Eyes with PEX syndrome had significantly lower cell densities in the basal epithelium ($P = 0.003$), anterior stroma ($P = 0.007$), intermediate stroma ($P = 0.009$), posterior stroma ($P = 0.012$), and endothelium ($P < 0.0001$) than in the corresponding layers of normal eyes. PEX eyes also had lower subbasal nerve densities and greater tortuosity of the nerves than normal eyes. Fellow eyes of patients with PEX also had significantly lower densities of the basal epithelial and endothelial cells than the normal eyes. Corneal sensitivity was significantly decreased in PEX eyes, and this was significantly correlated with the decrease of basal epithelial cell and subbasal nerve densities.

Conclusions. These results have shed light on understanding of the pathogenesis of decreased corneal sensitivity in eyes with PEX syndrome. PEX syndrome is probably a binocular condition for which keratopathy of the fellow eye also requires observation. (*Invest Ophthalmol Vis Sci.* 2011;52:1755–1761) DOI:10.1167/iovs.10-6098

The pseudoexfoliation (PEX) syndrome is a common age-related disorder of the extracellular matrix and is frequently associated with severe chronic secondary open angle glaucoma and cataract.[1–3] The prevalence of PEX syndrome varies widely in different racial and ethnic populations. In addition, the prevalence of PEX is dependent on the age and sex distribution of the population examined, the clinical criteria used to diagnose PEX, and the ability of the examiner to detect early stages and more subtle signs of PEX. For example, the highest rates in studies of persons older than 60 years of age have been reported to be approximately 25% in Iceland and more than 20% in Finland.[3,4] The ocular manifestation of PEX syndrome is the production and progressive accumulation of abnormal extracellular fibrillar material in almost all the inner wall tissues of the anterior segment of the eye. This characteristic alteration predisposes the eye to a broad spectrum of intraocular complications including phacodonesis and lens subluxation, angle closure glaucoma, melanin dispersion, poor mydriasis, blood-aqueous barrier dysfunction, posterior synechiae, and other related complications.[1–3]

The PEX syndrome is associated with corneal endotheliopathy, and this has been suggested to be the cause of the so-called atypical non-guttata Fuchs endothelial dystrophy.[5,6] PEX endotheliopathy, a slowly progressing disease of the corneal endothelium, is usually bilateral but is often asymmetrical. It can lead to early corneal endothelial cell decompensation, which can then induce severe bullous keratopathy, a vision-threatening disorder.

Clinical signs of PEX syndrome include decreased corneal sensitivity, thinning of the central corneal thickness, and impaired tear film stability.[7–9] However, the underlying cause of these clinical findings has not been well investigated, possibly because objective and accurate in vivo examination techniques are not available.

Recent advances in imaging technology have improved the ability of these instruments to diagnose different ocular diseases. The Rostock Cornea Module (Heidelberg Engineering, Heidelberg, Germany), consisting of a contact lens system attached to the Heidelberg Retina Tomograph II (Heidelberg Engineering), is such an instrument. It uses laser scanning technology to investigate the cornea at a cellular level, and structures such as the subbasal nerve plexus, which cannot be seen by slit-lamp microscopy, can be clearly seen.[10,11]

In vivo confocal microscopy (IVCM) was used by Martone et al.[12] to examine one eye with PEX syndrome, and noncontact IVCM was used by Sbeity et al.[13] to study PEX, PEX-suspect, and normal eyes. However, there has not been a detailed and quantitative study of the morphologic changes in the corneas of eyes with PEX syndrome.

Thus, the purpose of this study was to examine the underlying pathogenesis of PEX keratopathy and to obtain evidence to explain clinical findings such as the decreased corneal sensitivities observed in patients with PEX syndrome. To accomplish this, we used IVCM to determine cell densities in different corneal layers of eyes with PEX syndrome and their clinically unaffected fellow eyes. These findings were compared with those in normal control eyes. The nerve densities in the subbasal layer were also analyzed, and their relationship with the alterations of clinical corneal sensitivity were analyzed.

From the [1]Department of Ophthalmology, Ehime University School of Medicine, Ehime, Japan; [2]Department of Ophthalmology, Takanoko Hospital, Ehime, Japan; [3]Department of Ophthalmology, Red Cross Hospital in Matsuyama, Ehime, Japan; and [4]Department of Information Engineering, University of Padua, Padua, Italy.

Submitted for publication June 22, 2010; revised October 8, 2010; accepted November 1, 2010.

Disclosure: **X. Zheng**, None; **A. Shiraishi**, None; **S. Okuma**, None; **S. Mizoue**, None; **T. Goto**, None; **S. Kawasaki**, None; **T. Uno**, None; **T. Miyoshi**, None; **A. Ruggeri**, None; **Y. Ohashi**, None

Corresponding author: Xiaodong Zheng, Department of Ophthalmology, Ehime University School of Medicine, Toon City, Ehime 791-0295, Japan; xzheng@m.ehime-u.ac.jp.

Subjects and Methods

Subjects

We studied 27 patients (16 men, 11 women; mean age, 74.4 ± 6.3 years; age range, 65–90 years) with diagnoses of unilateral PEX syndrome. In all eyes, exfoliation material (XFM) was seen by slit-lamp microscopy at the pupillary border or on the anterior lens capsule. Eyes with PEX syndrome were placed in the PEX group, and clinically normal fellow eyes were placed in the PEX fellow eye group. Age- and sex-matched normal subjects (16 men, 11 women; mean age, 72.7 ± 6.5 years; age range, 61–92 years) were also studied. One eye from the normal control group was randomly selected and used in the statistical analyses. Exclusion criteria included Stevens-Johnson syndrome, lymphoma, sarcoidosis, corneal dystrophy, injury, inflammation, systemic therapy with drugs with known corneal toxicity; treatment with topical anti-glaucoma drugs, steroids, or NSAIDs; contact lens wear; previous ocular surgery; and other ophthalmic diseases.

The procedures used conformed to the tenets of the Declaration of Helsinki. Informed consent was obtained from all subjects after an explanation of the nature and possible consequences of the procedures. The protocol used was approved by the Ethics Committee of Ehime University School of Medicine.

Corneal Sensitivity Measurements

Measurement of the corneal sensitivity was performed with a Cochet-Bonnet nylon thread esthesiometer, as described.[14] The examination was begun with a 60-mm length of nylon filament applied perpendicularly to the central cornea, and the tests were continued by shortening the filament by 5 mm each time until the subject felt the contact of the filament. Each subject was measured twice with a between-test interval of at least 5 minutes, and the average of two measurements was used for the statistical analyses.

In Vivo Confocal Microscopy

IVCM was performed on all subjects with the Rostock Corneal Module of the Heidelberg Retina Tomograph II (HRTII-RCM; Heidelberg Engineering). After topical anesthesia with 0.4% oxybuprocaine (Santen Pharmaceuticals, Osaka, Japan), the subject was positioned in the chin and forehead holder and instructed to look straight ahead at a target to make sure that the central cornea was scanned. The objective of the microscope was an immersion lens (magnification ×63; Zeiss, Chester, VA) covered by a polymethylmethacrylate cap (TomoCap; Heidelberg Engineering). Comfort gel (Bausch & Lomb, Berlin, Germany) was used to couple the applanating lens cap to the cornea. The polymethylmethacrylate cap was applanated onto the center of the cornea by adjusting the controller, and in vivo digital images of the cornea were seen on the monitor screen. When the first layer of superficial epithelial cells was seen, the digital micrometer gauge was set to zero, and then a sequence of images was recorded as the focal plane was gradually moved toward the endothelium. Each subject underwent scanning three times at intervals of at least 15 minutes.

The laser source of the HRT-II RCM is a diode laser with a wavelength of 670 nm. Two-dimensional images consisting of 384 × 384 pixels covering an area of 400 × 400 μm were recorded. The digital resolution was 1.04 μm/pixel transversally and 2 μm/pixel longitudinally, as stated by the manufacturer.

Image Analyses

Central corneal images of all subjects were taken, and the three best-focused images from the superficial epithelium, basal epithelium, subbasal nerve plexus, anterior stroma, intermediate stroma, posterior stroma, and endothelium were selected for analyses. The selected images were randomly presented to two masked observers (XZ, SO) for evaluation. All data are presented as averages of three images.

Cell Density Analyses

Morphologic characteristics and densities in the different layers of the cornea in the PEX and PEX fellow eyes were assessed and compared with those of normal controls. Superficial epithelial cells were identified as polygonal cells with clearly visible cell borders, bright cytoplasm, and dark nuclei. Basal epithelial cells were identified as the layer just above the amorphous-appearing Bowman membrane. Basal cells had bright borders, a uniform shape, and nonhomogeneous cytoplasm. The anterior stroma was identified as the first layer immediately beneath the Bowman membrane, and the posterior stroma was identified as the layer just anterior to the Descemet membrane and the endothelium. The intermediate stroma was defined as the layer halfway between the anterior and posterior stroma.[15] The corneal endothelium consisted of a monolayer of regularly arranged hexagonal cells with dark borders and bright reflecting cytoplasm.

After selecting a frame of the image and manually marking the cells inside the frame (>50 cells), cell densities were calculated automatically by the software installed in the instrument. Cells partially contained in the area analyzed were counted only along the upper and right margins. The results are expressed in cells per square millimeter.

Analyses of Subbasal Nerve Plexus

The subbasal nerve plexus layer is located between the Bowman membrane and the basal epithelial layer through which numerous nerve fibers pass. The density and tortuosity of the subbasal nerve plexus were analyzed as described.[14,16] Two parameters were analyzed: the long nerve fiber density (LNFD) was determined by dividing the number of long nerves by the image area (0.16 mm^2), and the nerve branch density (NBD) was determined by dividing the total number of long nerves and their branches by the image area. Nerve tortuosity was classified into 4 gradings: grade 1 = approximately straight nerves; grade 4 = very tortuous nerves with significant convolutions throughout their course.[16]

Statistical Analyses

Data were analyzed with statistical software (JMP, version 8.0 for Windows; SAS Japan Inc., Tokyo, Japan). All data are expressed as the mean ± SD. The differences of cell densities between PEX eyes and normal controls or between PEX fellow eyes and normal controls were evaluated with two-tailed Student's *t*-tests. The differences of cell densities between PEX eyes and their fellow eyes were evaluated by paired *t*-tests. The Wilcoxon rank sum test was used to compare the values of corneal sensitivity, LNFD, NBD, and the nerve tortuosity between PEX patients and normal controls. Spearman's correlation was used to determine the correlation among the parameters of basal epithelial cell density, subbasal nerve density, and corneal sensitivity. $P < 0.05$ was considered statistically significant.

Results

The mean age was not significantly different between patients with PEX and normal controls (two-tailed Student's *t*-tests, $P = 0.725$). Eyes with PEX showed typical whitish exfoliation material on the pupillary border or on the anterior lens capsule on slit-lamp examination. Pigmented keratoprecipitates and slight folding of Descemet membrane were also detected in some patients. Fellow eyes of PEX eyes and normal control eyes appeared normal by slit-lamp microscopy.

Corneal Sensitivity

The mean corneal sensitivity was 47.8 ± 5.6 mm for PEX eyes and 53.7 ± 4.9 mm for PEX fellow eyes. This difference was significant ($P = 0.005$; Wilcoxon rank sum test). Mean corneal

sensitivity was 55.6 ± 4.7 mm for the normal control subjects, and the corneas of eyes with PEX were significantly less sensitive than those of normal control eyes ($P < 0.0001$). The difference in corneal sensitivity between PEX fellow eyes and normal controls was not significant ($P = 0.378$).

Cell Densities

The density of the corneal superficial epithelial cells was 872.6 ± 95.3 cells/mm^2, and that for the basal epithelial cells was 4829.7 ± 462.1 cells/mm^2 in PEX eyes. Densities for the corresponding layers in PEX fellow eyes were 910.4 ± 80.8 cells/mm^2 and 4996.7 ± 438.7 cells/mm^2, and densities for the normal control eyes were 886.4 ± 101.7 cells/mm^2 and 5446.4 ± 639.9 cells/mm^2. The density of the basal epithelial cells was significantly lower for PEX eyes and PEX fellow eyes than for the control eyes ($P = 0.003$ and $P = 0.015$, respectively; two-tailed Student's *t*-tests; Fig. 1). The difference in the density of the basal epithelial cells between PEX eyes and PEX fellow eyes was not significant ($P = 0.589$; paired *t*-test). Differences in the densities of the superficial epithelial cells among the three experimental groups also were not significant (Fig. 1).

Densities of the cells in the three stromal layers of PEX eyes, PEX fellow eyes, and normal control eyes are shown in Figure 2. Compared with normal controls, the cell densities of PEX eyes were significantly lower in all three layers of the stroma (anterior stroma, $P = 0.007$; intermediate stroma, $P = 0.009$; posterior stroma, $P = 0.012$; two-tailed Student's *t*-tests). The densities in these three stromal layers in PEX fellow eyes were also lower, but the decrease was not significant ($P = 0.196$; $P = 0.261$; $P = 0.08$; respectively; Fig. 2).

Endothelial cell densities were 2240.7 ± 236.6 cells/mm^2, 2386.6 ± 200.8 cells/mm^2, and 2738.7 ± 233.2 cells/mm^2 for PEX eyes, PEX fellow eyes, and normal eyes, respectively. Differences between PEX eyes and normal controls ($P < 0.0001$; two-tailed Student's *t*-test; Fig. 1) and between PEX fellow eyes and normal controls were significant ($P = 0.001$). The difference in endothelial cell density between PEX and PEX fellow eyes was not significant ($P = 0.754$; paired *t*-test).

There was a higher degree of pleomorphism and polymegethism in PEX eyes than in control eyes. The coefficient of variation (CV) of the cell area was 45.2% ± 8.7%, and the percentage of hexagonal cells (HEX) in PEX eyes was 30.5% ± 10.3%. Both values are significantly different from those of normal control eyes (CV, 30.6% ± 5.6%, $P = 0.016$; HEX, 50.3 ± 6.8%, $P = 0.008$; two-tailed Student's *t*-test). PEX fellow eyes also showed a similar tendency of increased pleomorphism and polymegethism, but the differences were not statistically significant.

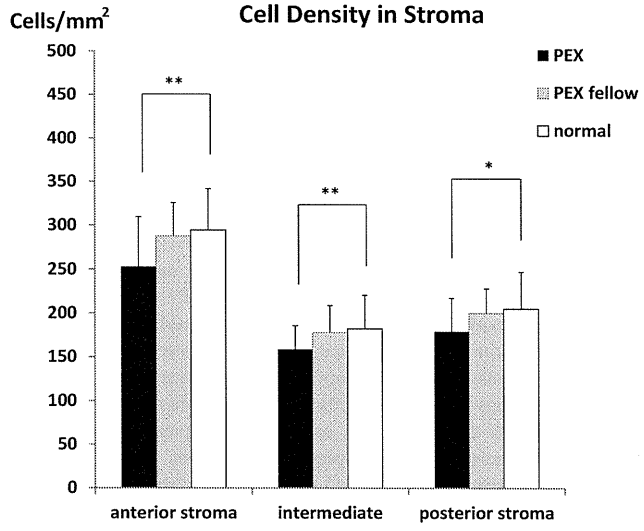

FIGURE 2. Cellular densities of anterior, intermediate and posterior stroma of eyes with PEX syndrome, their clinically unaffected fellow eyes, and eyes of normal control subjects. $^{**}P < 0.01$; $^{*}P < 0.05$.

Subbasal Nerve Plexus

The LNFD and NBD were significantly decreased in PEX eyes (17.4 ± 6.3 and 32.2 ± 8.3 nerves/mm^2, respectively) compared with those in normal controls (35.9 ± 8.2 and 72.2 ± 8.8 nerves/mm^2; $P < 0.0001$ and $P < 0.0001$, respectively; Wilcoxon rank sum test; Fig. 3). PEX fellow eyes also had decreased LNFD and NBD, but these changes were not

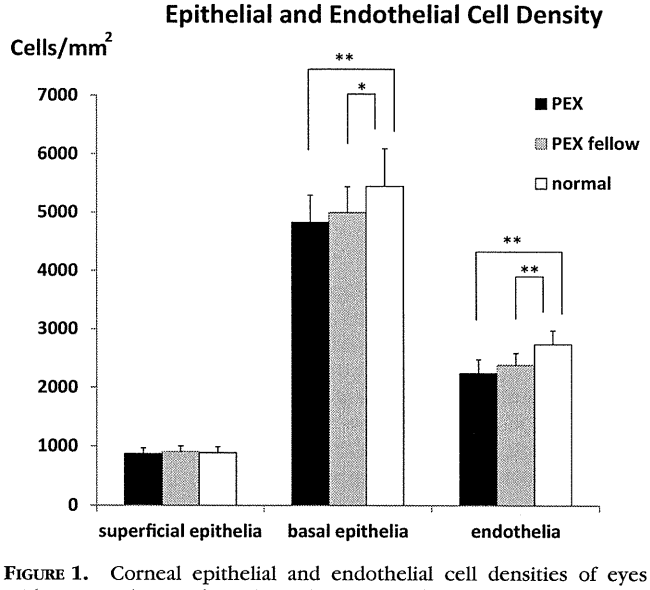

FIGURE 1. Corneal epithelial and endothelial cell densities of eyes with PEX syndrome, their clinically unaffected fellow eyes, and eyes of normal control subjects. $^{**}P < 0.01$; $^{*}P < 0.05$.

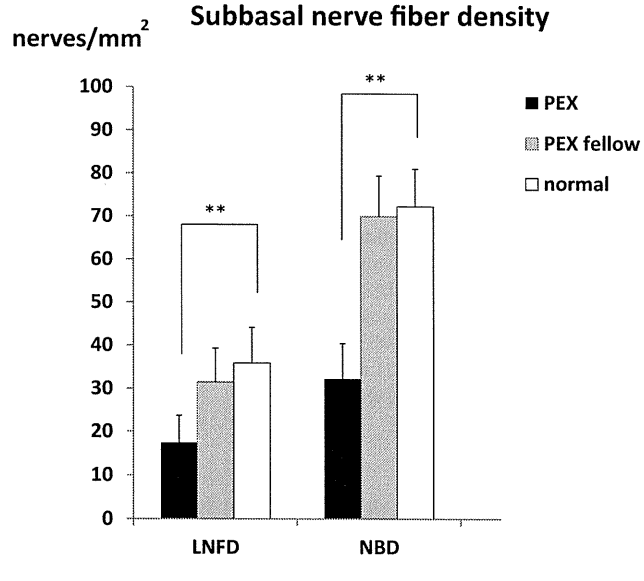

FIGURE 3. Subbasal LNFD and NBD in eyes with PEX syndrome, their clinically unaffected fellow eyes, and eyes of normal control subjects. $^{**}P < 0.01$.

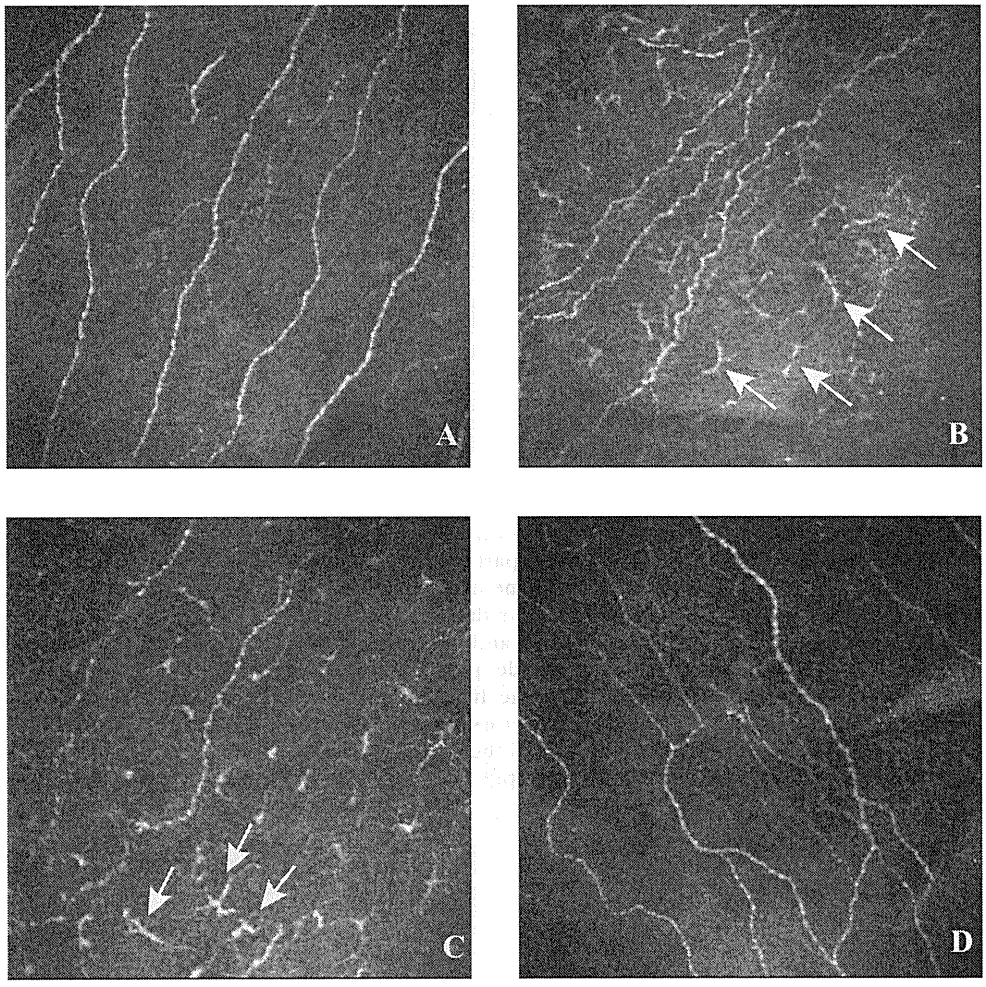

FIGURE 4. In vivo confocal microscopic images of the subbasal nerve plexus in patients with PEX syndrome and a normal control subject. (**A**) Representative image from a normal control subject showing subbasal nerve plexus with long nerve fibers running parallel to the Bowman layer. The nerve fibers appeared to be straight with minimal tortuosity. The subbasal LNFD was 31.3 nerves/mm^2, and the nerve tortuosity was grade 1. (**B**) Representative image from a PEX syndrome eye showing very tortuous nerves with significant convolutions throughout their course. The tortuosity grade was 4. Note the intensive infiltration of dendritic cells (*arrows*) in close vicinity of the nerve fibers. (**C**) Confocal image of the subbasal nerve plexus of another PEX eye showing the thinning of the nerves, short nerve sprouts, fewer branches from the main nerve trunk, and significantly decreased nerve density. The LNFD was 6.3 nerves/mm^2. *Arrows*: dendritic cell infiltration. (**D**) Confocal image of a PEX fellow eye showing moderately tortuous subbasal nerve plexus with a tortuosity grade of 3 and an LNFD of 18.8.

significantly different from those of the controls (31.5 ± 7.8 and 69.9±9.4 nerves/mm^2; $P = 0.093$ and $P = 0.301$).

Confocal images of PEX eyes showed extremely tortuous nerve fibers, thinning of nerves, short nerve sprouts, fewer branches from the main nerve trunk, and highly reflective inflammatory infiltrates in close vicinity of the subbasal nerves. Representative confocal images of the three groups are shown in Figure 4. In PEX eyes, 85.2% (23 of 27 eyes) had grade ≥3 subbasal nerve tortuosity, and the degree of tortuosity in PEX eyes was significantly higher than that of the controls (3.2 ± 0.7 vs. 1.6 ± 0.6; $P < 0.0001$; Wilcoxon rank sum test). The degree of tortuosity in PEX fellow eyes was also greater than that of normal controls, although the difference was not significant (2.1 ± 0.9 vs. 1.6 ± 0.6; $P = 0.054$).

It was our impression that PEX eyes had more inflammatory cells, including dendritic cells, infiltrating the subbasal cell layer and anterior stroma, and these changes were more severe in eyes with decreased subbasal nerve densities and lower corneal sensitivities (Fig. 4).

Correlation between Corneal Sensitivity and Subbasal Nerve Density and Basal Epithelial Cell Density

Spearman's correlation analyses showed that there was a significant positive correlation between corneal sensitivity and the subbasal nerve densities (LNFD, $r = 0.764$, $P < 0.0001$; NBD, $r = 0.634$, $P < 0.0001$; Spearman correlation coefficient). Corneal sensitivity was also significantly and positively correlated with basal epithelial cell density and significantly and negatively correlated with subbasal nerve tortuosity (Table 1).

Confocal Microscopic Detection of Hyperreflective Material

IVCM showed hyperreflective material, probably XFM, in the subbasal epithelial layer or the anterior stroma of 22 of the 27 PEX eyes (81.5%). The hyperreflective material was also observed abundantly in the endothelia of all PEX eyes. Five of 27 (18.5%) PEX fellow eyes showed hyperreflective deposits in the subbasal epithelial layer or anterior stroma, and 14 of 27 (51.9%) had endothelial surface deposits of hyperreflective material. In sharp contrast, none of the normal eyes showed hyperreflective material in the subbasal epithelial or anterior

TABLE 1. Correlation among Corneal Sensitivity, Subbasal Nerve Fiber Density, Tortuosity, and Basal Epithelial Cell Density

	Corneal Sensitivity	
	Spearman Correlation Coefficient	*P*
Long nerve fiber density	0.7640	<0.0001*
Nerve branch density	0.6341	<0.0001*
Subbasal nerve fiber tortuosity	−0.8250	<0.0001*
Basal epithelial cell density	0.6971	<0.0001*

* Statistically significant.

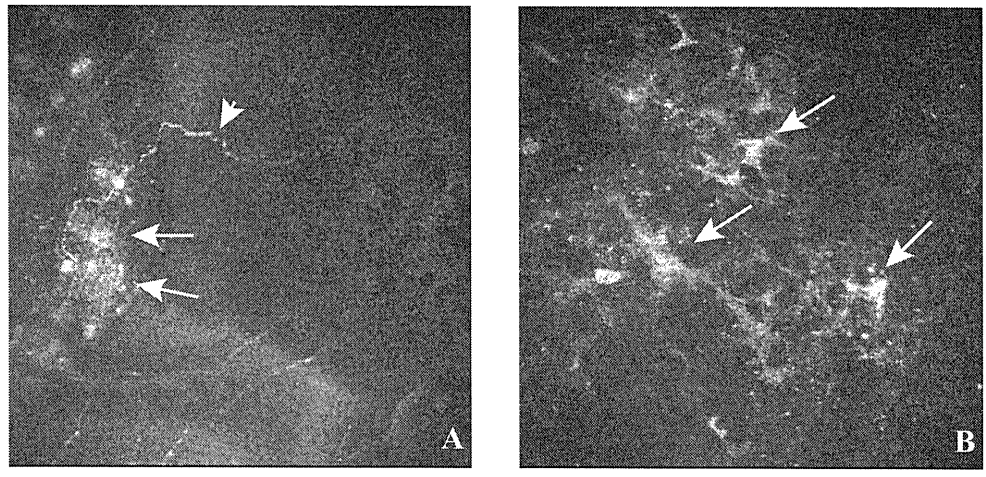

FIGURE 5. Confocal microscopic images showing XFM in the subbasal nerve plexus layer of a patient with PEX syndrome. (**A**) Nerve fiber thinning with tortuous morphology can be seen (*arrowhead*), and XFM (*arrows*) is seen in close vicinity of the pathogenic nerve fibers. (**B**) Hyperreflective deposits (*arrows*) indicative of XFM can be seen in the subbasal amorphous layer of the cornea of another patient in the PEX eye group.

stromal layers, and only two (7.4%) had a small amount of hyperreflective material on the endothelial surface (Figs. 5, 6).

DISCUSSION

The manifestations of PEX syndrome in the anterior segment are widely known to affect intraocular surgery with poor mydriasis and intensive postoperative inflammation. The fact that aggregates of XFM can be identified in autopsy specimens of the heart, lung, liver, kidney, and other organs in patients with ocular PEX suggests that the ocular PEX syndrome is part of a general systemic disorder.[1-3,17] In fact, PEX syndrome has been reported to be associated with cardiovascular diseases, chronic cerebral disorders, Alzheimer disease, and acute cerebrovascular events.[1-3] Two single nucleotide polymorphisms in the lysyl oxidase-like 1 (*LOXL1*) gene have been recently identified as strong genetic risk factors for PEX syndrome and PEX glaucoma.[18]

IVCM with the HRTII-RCM provides a new imaging method that allows rapid, noninvasive, high-resolution, and microstruc-

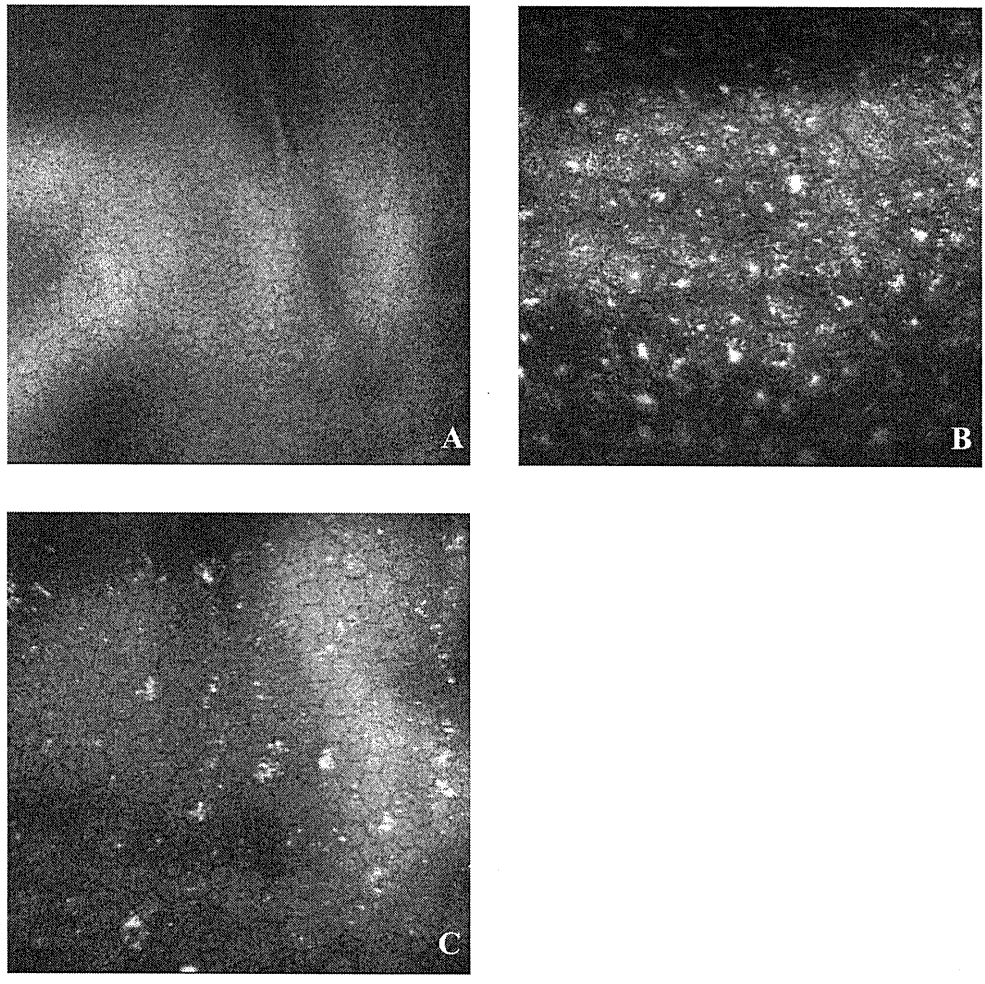

FIGURE 6. Representative confocal microscopic images of the endothelial layers of PEX syndrome eye, PEX fellow eye, and normal control eye group. (**A**) Normal subject with regularly arranged hexagonal endothelial cells. (**B**) PEX eye showing increases in pleomorphism and polymegethism and decrease in cell density. Intense hyperreflective materials indicative of XFM can be seen. (**C**) PEX fellow eye showing similar changes of endothelial cells and deposition of XFM.

tural examination of the cornea.[10,11] Only two studies have used IVCM to study the corneas of patients with PEX syndrome. Martone et al.[12] reported the findings in one case, and they reported that ICVM can detect hyperreflective deposits and dendritic cells infiltrating the basal epithelial cell layer. Fibrillar subepithelial structures were found, and the endothelial layer showed cellular anomalies. In a prospective observational case series, Sbeity et al.[13] used noncontact IVCM to detect XFM on the lens surfaces and corneal endothelia of PEX eyes and their fellow eyes.

Our study was the first to use IVCM to investigate cell densities in different layers of the cornea and to determine alterations of subbasal nerve density and tortuosity in PEX and PEX fellow eyes. Our results showed a significant decrease in the densities of the corneal endothelial cells in PEX eyes and their fellow eyes, which is in agreement with earlier observations by specular microscopy.[8,19,20] In addition, the clear confocal images allowed us to detect pleomorphisms and polymegethisms of the endothelial cells. All PEX eyes and 51.9% of PEX fellow eyes showed deposits of hyperreflective material in the endothelium, indicative of either pigment granules or XFM. In agreement with Sbeity et al.,[13] we believe that the pleomorphic and irregular deposits found on the corneal endothelium most likely represent XFM rather than pigment granules, which are round and uniform in size.[13] In addition, a number of patients who had no visible pigment keratoprecipitates on slit-lamp microscopy were found to have abundant large and irregular hyperreflective deposits on the endothelium in the confocal images.

PEX syndrome–associated corneal endotheliopathy has been suggested to be caused by one or a combination of the following alterations: hypoxic changes in the anterior chamber, accumulation of extracellular matrix, fibroblastic changes of the endothelium, and increased concentration of TGF-β.[1-3] Our confocal microscopic findings suggest that the XFM, possibly at different stages of the normal course of PEX, may be deposited on the endothelium or may migrate from the endothelial cells that undergo fibroblastic changes. Our findings also showed that hyperreflective materials are found not only on the endothelium of PEX eyes but also in their fellow eyes, indicating that the fellow eyes might be at a preclinical stage of PEX syndrome. A bilateral decrease in the endothelial cell counts and morphologic alterations of endothelium support the idea that PEX is a binocular and systemic abnormality. Patients with unilateral PEX syndrome may have asymmetric manifestation of this slowly progressing disease.

Of clinical significance was our finding that the decreased stromal cell densities observed by IVCM could possibly explain the report that the central corneas of PEX eyes were thinner than those of normal subjects.[8] The pathogenesis of the decrease of stromal cell density in PEX eyes warrants future study. Because XFM deposits were simultaneously observed in the anterior stroma of PEX eyes, we suggest that the XFM may be somehow causative for this alteration, perhaps by inducing apoptosis of the keratocytes. Other pathogenic factors, such as altered levels of cytokines or chemokines in the cornea, could also be responsible, and this definitely warrants future investigation. In addition, PEX fellow eyes also had lower cell counts in the stroma, although the difference was not statistically significant. We suggest that the cause of the binocular differences in our study might have been because the two eyes were at different stages of the PEX process, and PEX fellow eyes may still be at a preclinical stage of PEX syndrome.

Other important findings were found in the subbasal nerve plexus. Our results showed that the subbasal nerve density was significantly lower and the nerves were mostly tortuous, with beading and thinning in PEX eyes. Interestingly, PEX fellow eyes also had similar alterations, though the changes were not significant. These findings support the idea that PEX syndrome is a binocular abnormality that is expressed in both eyes but to different degrees. The important clinical significance of our study is that our correlation analyses showed that the decreased subbasal nerve density and increased tortuosity were significantly correlated with decreased corneal sensitivity. These results provide evidence, for the first time, that the cause of the decreased corneal sensitivity in eyes with PEX syndrome is the decreased subbasal nerve density. For patients with PEX syndrome, it would be practical and feasible to examine corneal sensitivity to assess the severity of PEX keratopathy and perhaps to predict the progression of PEX syndrome. In addition, detection of the morphologic changes in cell densities and subbasal nerve abnormalities by IVCM in the fellow eyes indicates that it is a sensitive tool for the diagnosis of preclinical stage of PEX syndrome. Our findings showed that PEX keratopathy may develop before any clinically visible XFM deposits are detected on the lens capsule or iris. If these findings are confirmed, then keratopathy may be the first event of the ocular complications of PEX syndrome. These findings also indicate that clinically unaffected fellow eyes of patients with PEX syndrome are probably at risk for PEX syndrome, and more frequent ophthalmologic examinations are necessary.

This study has increased our understanding of the keratopathy of this most likely systemic abnormality. Whether the alternations of the subbasal corneal nerves are primary or secondary changes of the disease must be determined. Because of the increase in the elastic microfibril components and imbalances in the matrix metalloproteinases (MMPs) and tissue inhibitors of MMP in eyes with PEX syndrome, PEX fibrils accumulate in the tissues.[1-3] Our findings that XFM deposits were frequently observed close to the subbasal epithelial layer or anterior stroma support the idea that besides an abnormal aggregation of elastic microfibrils into exfoliation fibers (the elastic microfibril hypothesis),[1-3,21] other extracellular matrix components, such as basement membrane components, may possibly interact and become incorporated into the composite XFM (the basement membrane hypothesis).[2,3] In addition, our observation of an infiltration of dendritic cells in close vicinity of the subbasal nerve plexus layer indicates the possibility that accumulation of extracellular XFM may induce inflammatory responses, which then recruit antigen-presenting cells such as immunocompetent dendritic cells. This excessive deposition of XFM and infiltration of dendritic cells may play a role in the neuropathy of the subbasal nerve plexus, resulting in decreased corneal sensitivity in patients with PEX syndrome.

Some limitations were present this study. First, the IVCM scans a very small area of the cornea, which may generate biases among different portions of scanning of different groups. As mentioned, efforts were taken to scan the center of the cornea of each subject. In addition, we also confirmed our findings by scanning the midperipheral and peripheral portions of the cornea (data not shown).

Second, IVCM images may not represent the true histologic changes of the cornea. By applying the same criteria for image evaluation, we can conclude that the differences between the studied groups were still detected. Furthermore, it was our impression that fewer keratocytes were seen in the stromas of corneal specimens obtained from PEX syndrome patients with penetrating keratoplasty.

Future investigations, including a thorough and quantitative analysis of the exfoliation material by confocal imaging, are needed. In addition, the correlations between IVCM findings with endothelial barrier function should be determined. If the confocal findings can provide clues for preclinical stages of endothelial barrier dysfunction of the cornea in PEX syndrome, their clinical significance can be used in designing an early treatment protocol.